Targeting Apoptotic Pathways in Cancer: Design, Synthesis, and Molecular Docking studies of 1,3,5-Trisubstituted-1*H*-Pyrazole Derivatives with Bcl-2 Inhibition and DNA Damage Potential

Ahmed Temirak[a*], Ahmed A. F. Soliman[b], Mohamed B. Shalaby[c], Mariam G. Eshak[d], Wagdy K. B. Khalil[d], Zahid Shafiq[e], Nader M. Boshta[f*]

[a] Chemistry of Natural and Microbial Products Department, Pharmaceutical and Drug Industries Research Institute, National Research Centre, Dokki, Giza, 12622, Egypt.

[b] Drug Bioassay-Cell Culture Laboratory, Pharmacognosy Department, National Research Center, Giza 12622, Egypt.

[c] Toxicology Research Department, Research Institute of Medical Entomology (RIME), General Organisation of Teaching Hospitals and Institutes (GOTHI), Ministry of Health and Population (MoHP), Dokki, P.O. Box 12311, Cairo, Egypt.

[d] Department of Cell Biology, National Research Centre, 12262 El-Bohouth St., Cairo, Egypt.

[e] Institute of Chemical Sciences, Bahauddin Zakariya University, Multan, Pakistan.

[f] Chemistry Department, Faculty of Science, Menoufia University, Shebin El-Koam 32511, Egypt.

Corresponding authors:
Email address: Ahmed Temirak (amtemirak@hotmail.com), Nader M. Boshta (nboshta2@gmail.com).

Table of Contents

Contents	**Pages**
Visual score of DNA damage in MCF-7, A549 and PC3 cancer cell lines	**S2-S4**
Molecular docking experimental part	**S5**
^{1}H, ^{13}C-NMR spectra and LC-MS charts of the final compounds	**S6–S34**
References	**S35**

Table S1: Visual score of DNA damage in MCF-7 cancer cell lines treated with different compounds and Doxorubicin.

Treatment		No. of cells		Class**				DNA damaged cells % (Mean±SEM)
	No of samples	Analyzed*	Comets	0	1	2	3	
MCF-7 (-ve)	4	404	43	361	32	6	5	10.64 ± 0.85[c]
MCF-7 + **6c**	4	404	149	255	48	52	49	36.88 ± 1.38[a]
MCF-7 + **8**	4	404	84	320	35	27	22	20.79 ± 1.59[b]
MCF-7 + **10b**	4	404	141	263	51	46	44	34.90 ± 1.75[a]
MCF-7 + **10c**	4	404	96	308	32	35	29	23.76 ± 1.49[b]
MCF-7 + **Doxo**	4	404	153	251	41	54	58	37.87 ± 1.88[a]

*: Number of cells examined per a group, **: Class 0= no tail; 1= tail length < diameter of nucleus; 2= tail length between 1X and 2X the diameter of nucleus; and 3= tail length > 2X the diameter of nucleus. [a,b,c:] Mean values within tissue with unlike superscript letters were significantly different (P<0.05). Doxorubicin (Doxo).

Table S2: Visual score of DNA damage in A549 cancer cell lines treated with different compounds and Doxorubicin.

Treatment		No. of cells		Class**				DNA damaged cells % (Mean±SEM)
	No of samples	Analyzed*	Comets	0	1	2	3	
A549 (-ve)	4	404	42	362	31	7	4	10.40 ± 1.19^{d}
A549 + **6c**	4	404	126	278	46	49	31	31.19 ± 2.02^{ab}
A549 + **8**	4	404	79	325	34	25	20	19.55 ± 1.76^{c}
A549 + **10b**	4	404	115	289	45	49	21	28.47 ± 165^{b}
A549 + **10c**	4	404	89	315	30	35	24	22.03 ± 1.47^{c}
A549 + **Doxo**	4	404	135	269	43	50	42	33.42 ± 1.19^{a}

*: Number of cells examined per a group, **: Class 0= no tail; 1= tail length < diameter of nucleus; 2= tail length between 1X and 2X the diameter of nucleus; and 3= tail length > 2X the diameter of nucleus. $^{a,b,c,d:}$ Mean values within tissue with unlike superscript letters were significantly different (P<0.05). Doxorubicin (Doxo).

Table S3: Visual score of DNA damage in PC3 **cancer cell lines treated with different compounds and Doxorubicin.**

Treatment		**No. of cells**		**Class****				**DNA damaged cells % (Mean±SEM)**
	No of samples	**Analyzed***	**Comets**	**0**	**1**	**2**	**3**	
PC3 (-ve)	4	404	44	360	30	6	8	10.89 ± 0.85^{c}
PC3 + **6c**	4	404	93	311	31	29	33	23.02 ± 1.96^{a}
PC3 + **8**	4	404	75	329	33	24	18	18.56 ± 1.25^{b}
PC3 + **10b**	4	404	88	316	36	22	30	21.78 ± 1.11^{ab}
PC3 + **10c**	4	404	79	325	35	20	24	19.55 ± 1.85^{b}
PC3 + **Doxo**	4	404	99	305	34	28	37	24.50 ± 1.55^{a}

*: Number of cells examined per a group, **: Class 0= no tail; 1= tail length < diameter of nucleus; 2= tail length between 1X and 2X the diameter of nucleus; and 3= tail length > 2X the diameter of nucleus. $^{a,b,c:}$ Mean values within tissue with unlike superscript letters were significantly different (P<0.05). Doxorubicin (Doxo).

Molecular Docking

We conducted a molecular docking study to evaluate the potential anti-cancer effects of our newly developed 1,3,5-trisubstituted-1*H*-pyrazole derivatives (**6c**, **8**, **10b**, and **10c**) by targeting the Bcl-2 protein. This analysis included examining the binding modes and affinities of these compounds within the Bcl-2 protein's active sites. To begin, we obtained the X-ray crystal structures of the Bcl-2 protein from the Protein Data Bank (https://www.rcsb.org) using the PDB code 4AQ3.[1] The receptor preparation for docking was carried out using Biovia Discovery Studio,[2] which involved removing unnecessary chains and water molecules, adding polar hydrogens, and adjusting partial charges to create accurate receptor models suitable for docking simulations.

For the docking studies, we utilized the Autodock 4.2 software package. The process began with preparing coordinate files for both the ligands and the target protein, followed by the calculation of an affinity grid for the target. The grid box was set at dimensions of 50x50x50 with a grid point spacing of 0.375 Å, centered on the position of the co-crystallized ligand. The Lamarckian Genetic Algorithm (LGA) was employed to explore possible conformations, running ten iterations with up to 27,000 generations per iteration. The mutation rate was set at 0.02, and the crossover rate was 0.8. Multiple docking runs were performed using AutoDock 4.2[3] to generate a variety of docked conformations. The best docking results were determined by evaluating the predicted binding energies and the consistency of the docking poses.

^{1}H and ^{13}C NMR spectra for 3-(3,4-Dichlorophenyl)-5-(1-methyl-1*H*-pyrrol-2-yl) -4,5-dihydro-1*H*-pyrazole-1-carbothio-amide **(5).**

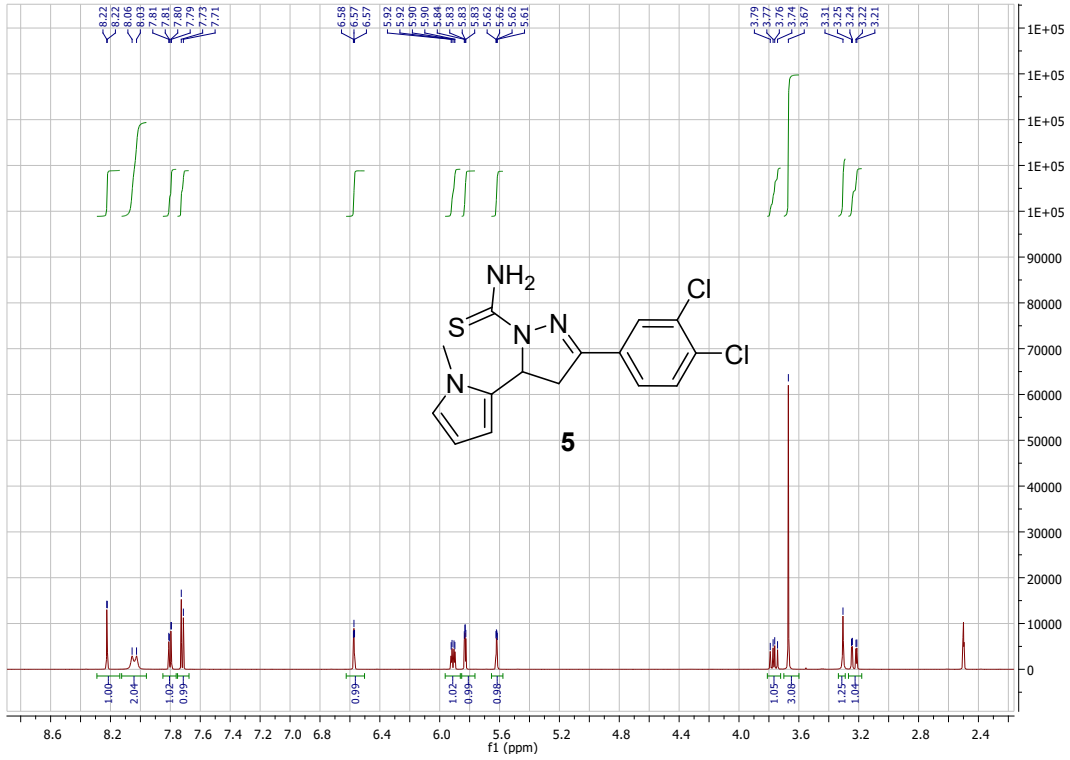

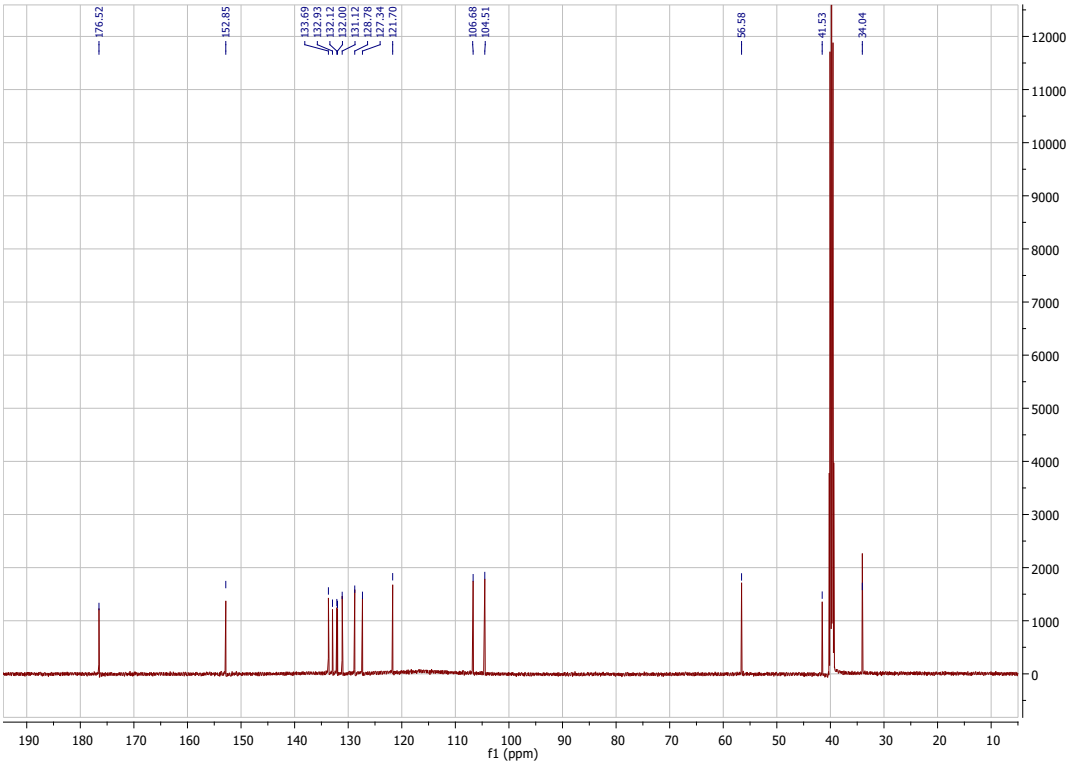

^{1}H and ^{13}C NMR spectra for 4-(4-Chlorophenyl)-2-(3-(3,4-dichlorophenyl)-5-(1- methyl-1*H*-pyrrol-2-yl)-4,5-dihydro-1*H*-pyrazol-1-yl)thiazole **(6a).**

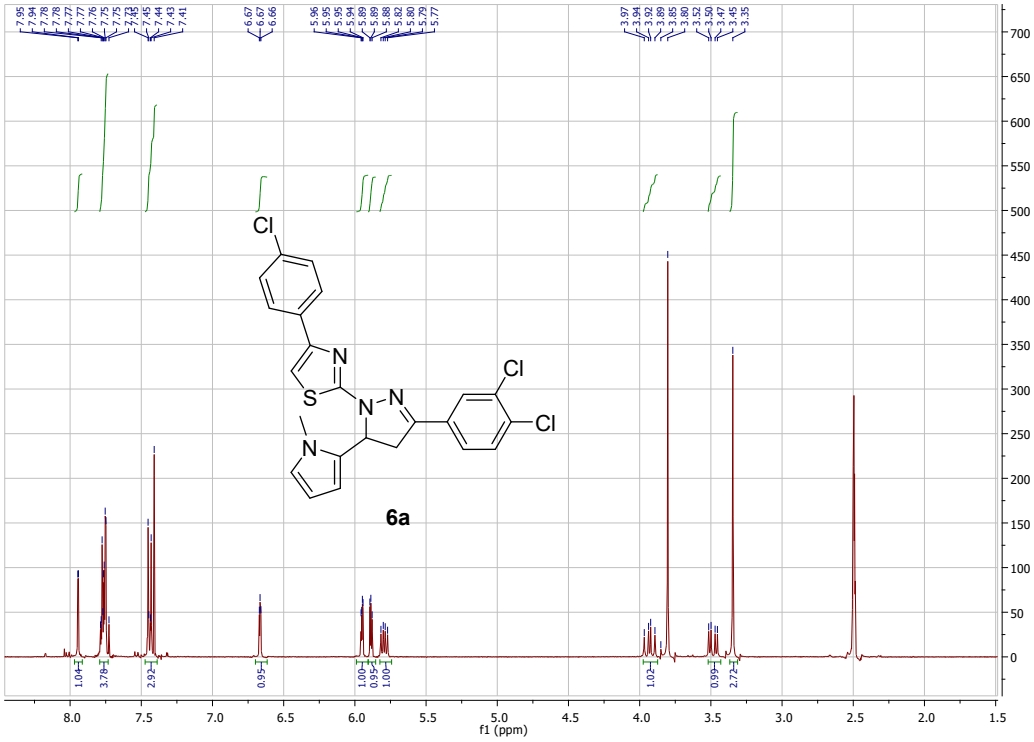

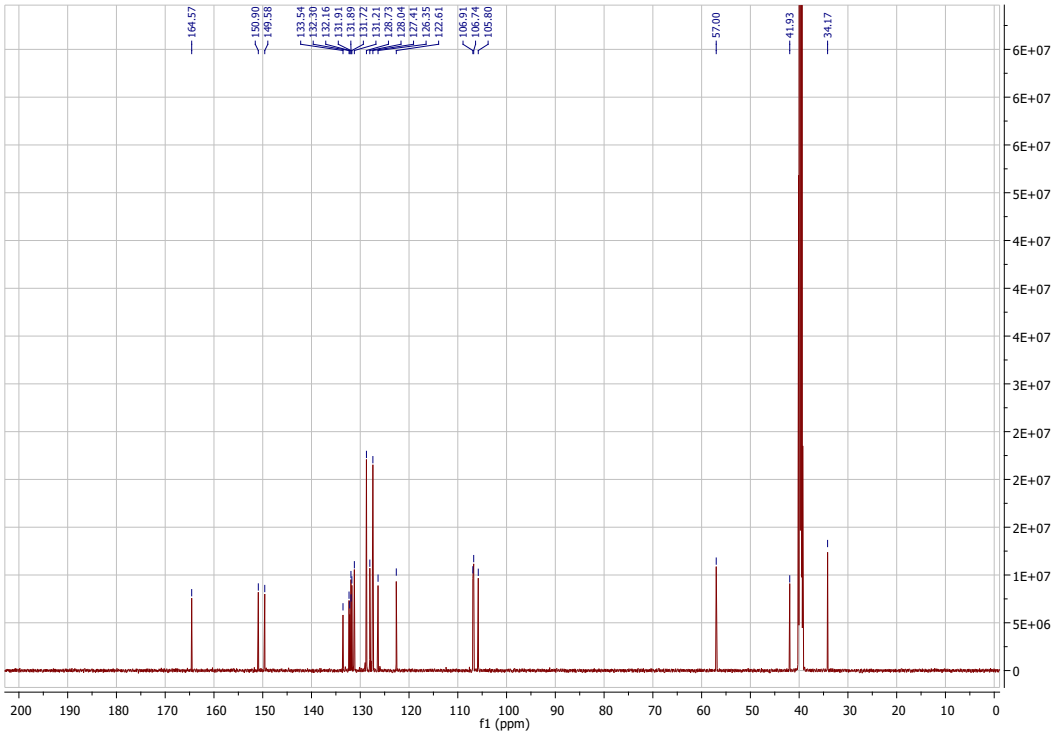

^{1}H and ^{13}C NMR spectra for 2-(3-(3,4-dichlorophenyl)-5-(1-methyl-1*H*-pyrrol -2-yl)-4,5-dihydro-1*H*-pyrazol-1-yl)-4-(2-methoxyphenyl)thiazole **(6b).**

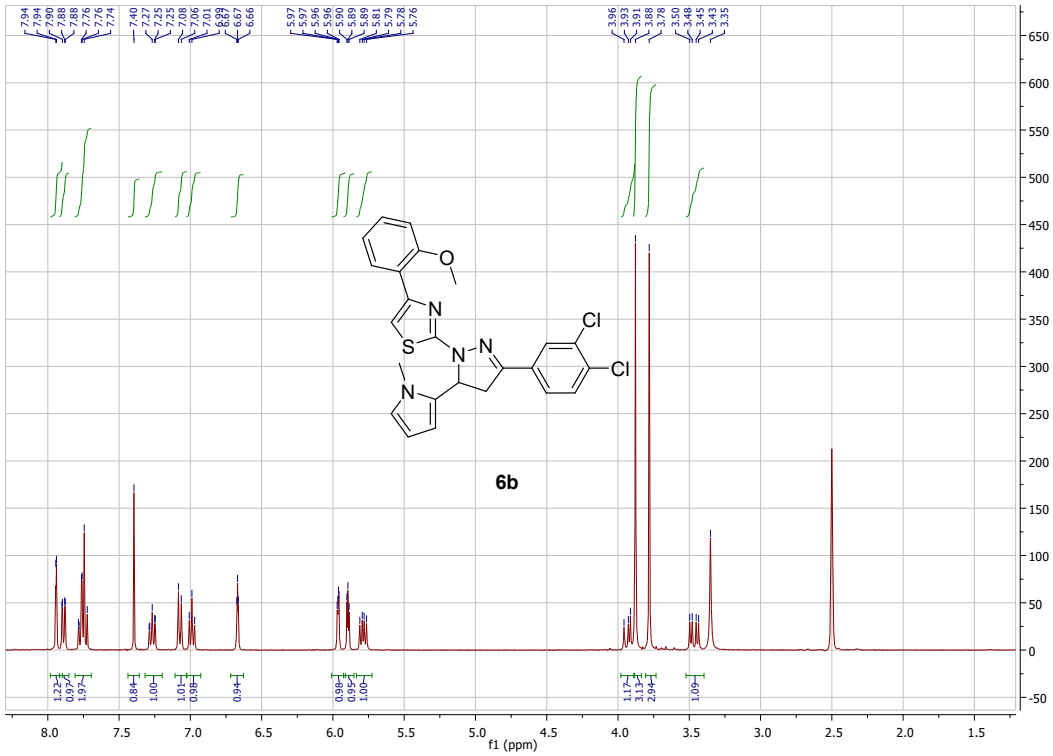

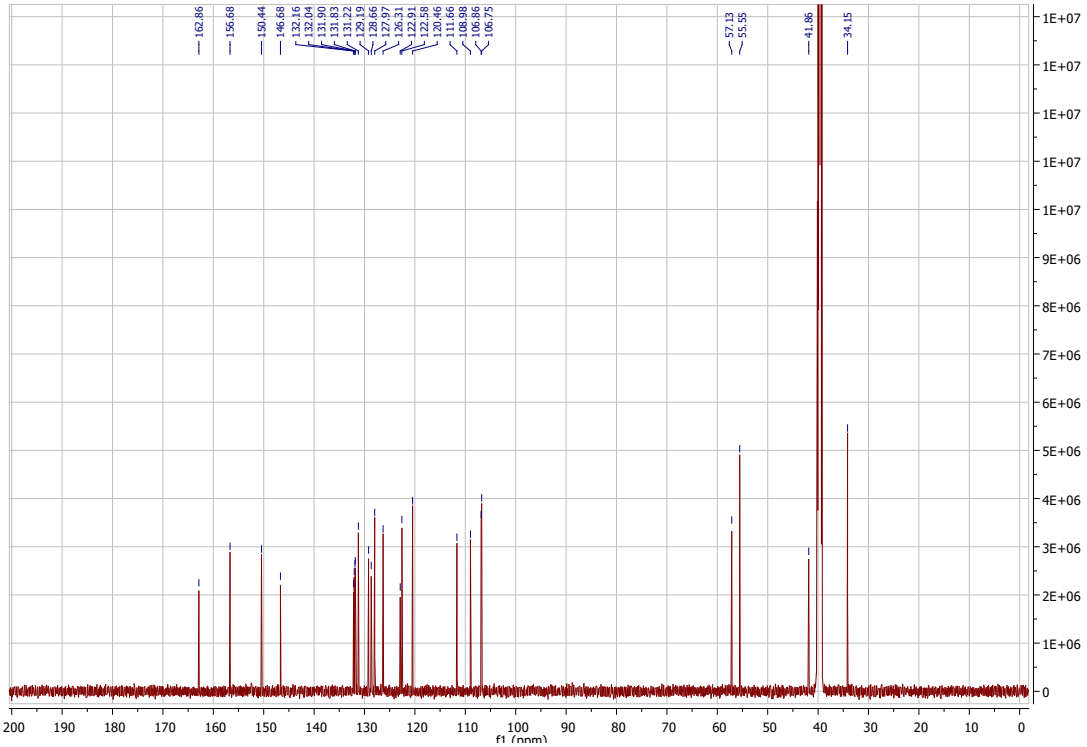

LCMS spectra for 2-(3-(3,4-dichlorophenyl)-5-(1-methyl-1*H*-pyrrol -2-yl)-4,5-dihydro-1*H*-pyrazol-1-yl)-4-(2-methoxyphenyl)thiazole **(6b).**

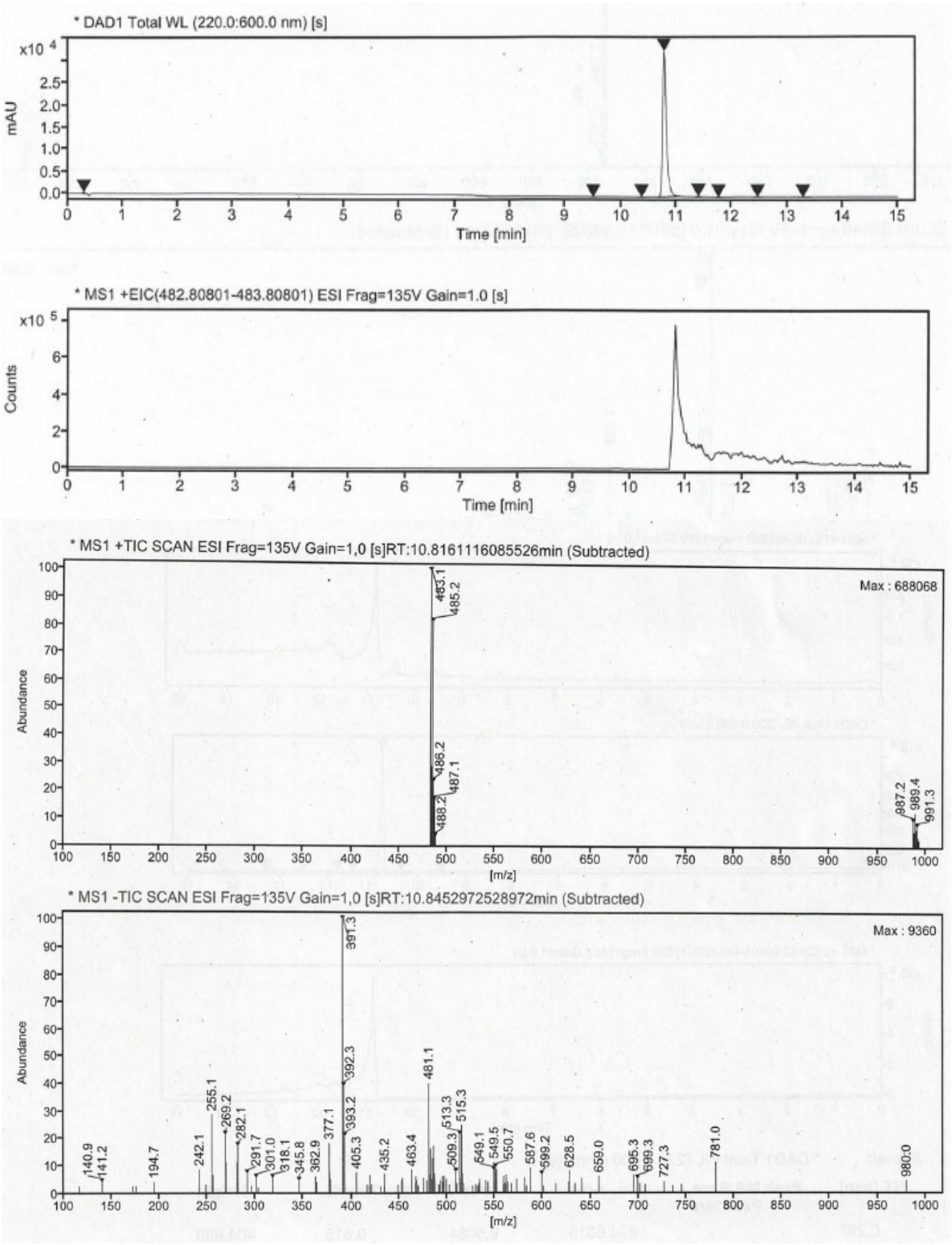

Signal: * DAD1 Total WL (220.0:600.0 nm) [s]

RT [min]	Peak MS Base Peak m/z	Area	Area%	Max Peak%	Height
0.297		824.8015	0.5084	0.515	404.699
9.501		127.6911	0.0787	0.080	29.453
10.374		227.8713	0.1405	0.142	53.436
10.781	391.300	160148.5776	98.7189	100.000	32786.771
11.404		606.7174	0.3740	0.379	158.842
11.764		67.3917	0.0415	0.042	18.900
12.467		141.6926	0.0873	0.088	29.364

^{1}H and ^{13}C NMR spectra for 2-(3-(3,4-dichlorophenyl)-5-(1-methyl-1*H*-pyrrol -2-yl)-4,5-dihydro-1*H*-pyrazol-1-yl)-4-(pyridin-4-yl)thiazole **(6c).**

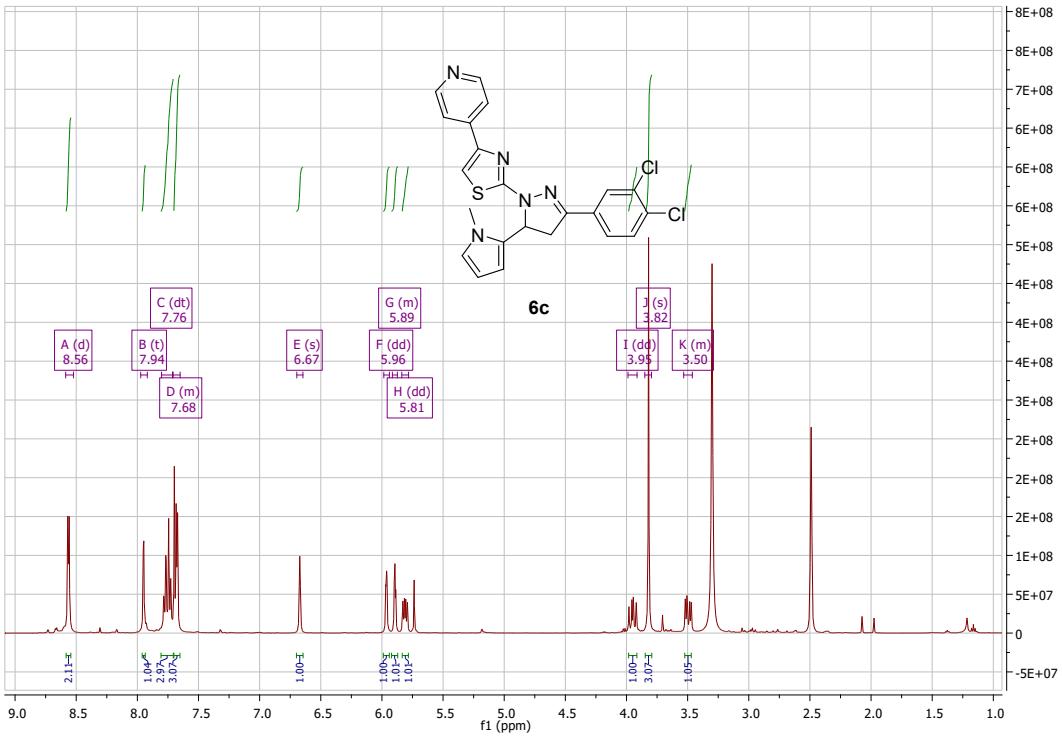

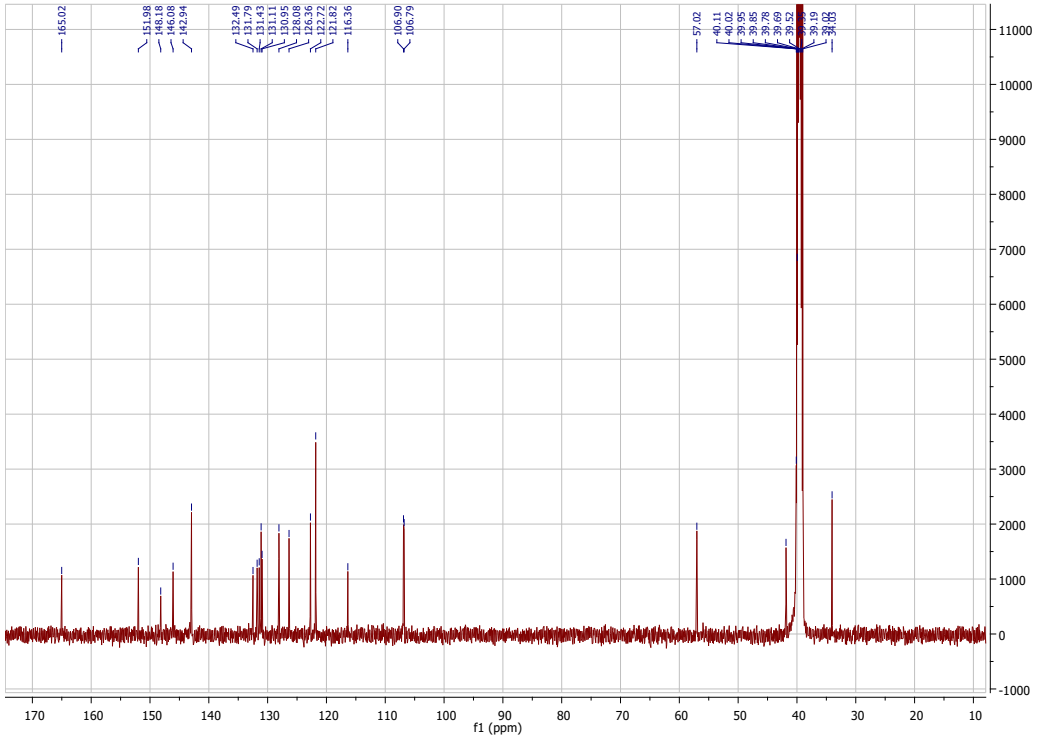

LC-MS for 2-(3-(3,4-dichlorophenyl)-5-(1-methyl-1*H*-pyrrol-2-yl)-4,5-dihydro-1*H*-pyrazol-1-

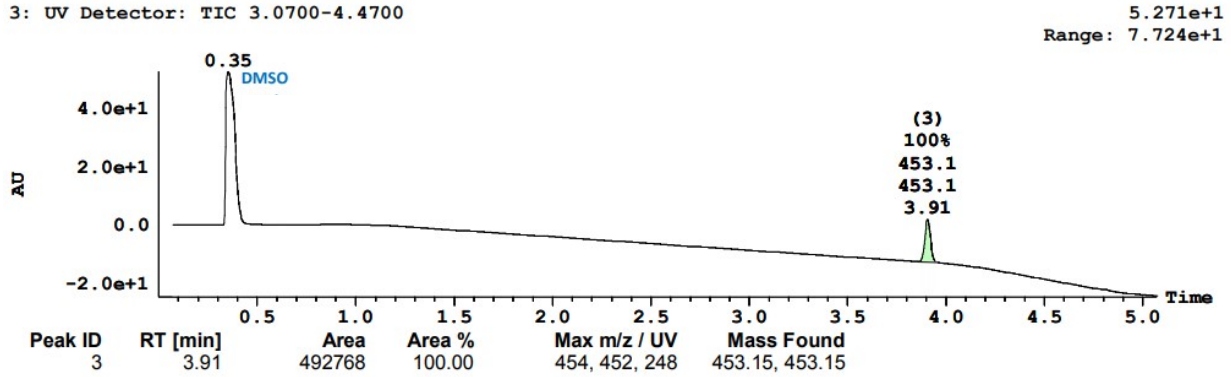

Peak ID	RT [min]	Area	Area %	Max m/z / UV	Mass Found
3	3.91	492768	100.00	454, 452, 248	453.15, 453.15

yl)-4-(pyridin-4-yl)thiazole **(6c)**.

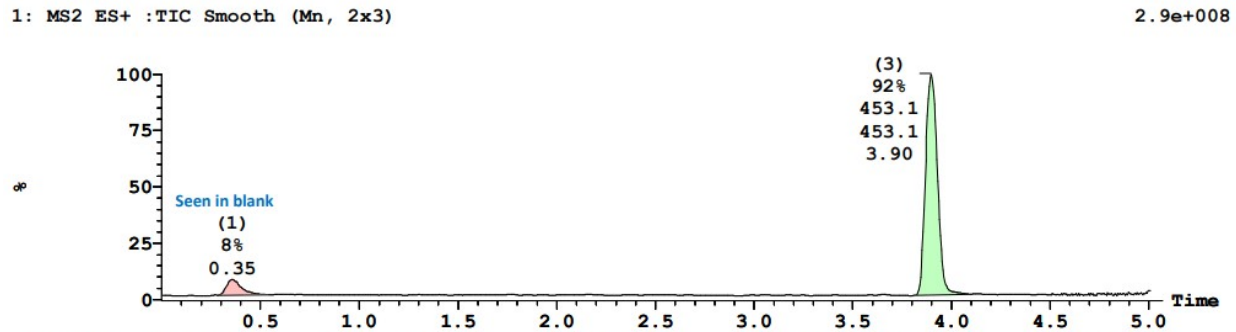

Peak ID	Rt [min]	Area	Area %	Max m/z / UV	Mass Found	Compd	State
1	0.35	1740024	8.06	135			Diversity fail
3	3.90	19853264	91.94	454, 452, 248	453.15, 453.15	Found	OK

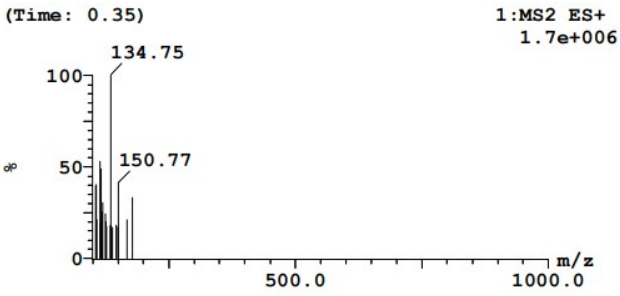

Peak ID	Target	Mass Found
3	452.1,408.1	452.14,

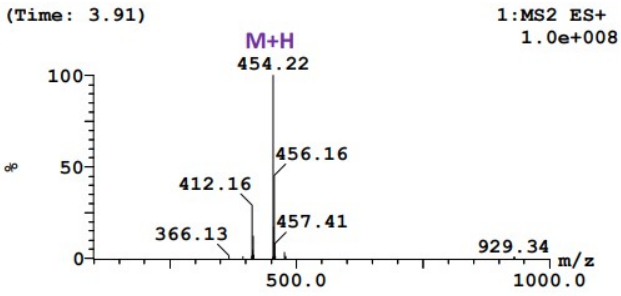

Peak ID	Target	Mass Found
3	No Target	

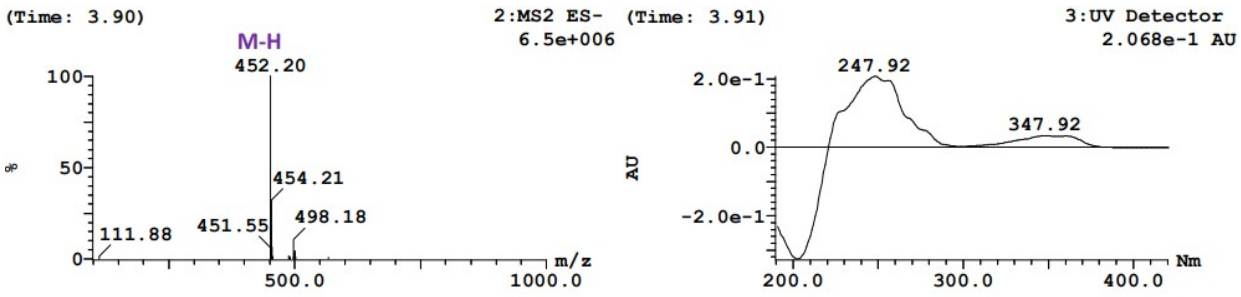

^{1}H and ^{13}C NMR spectra for 4-(2-chlorophenyl)-2-(3-(3,4-dichlorophenyl)-5-(1-methyl -1*H*-pyrrol-2-yl)-4,5-dihydro-1*H*-pyrazol-1-yl)thiazole **(6d)**.

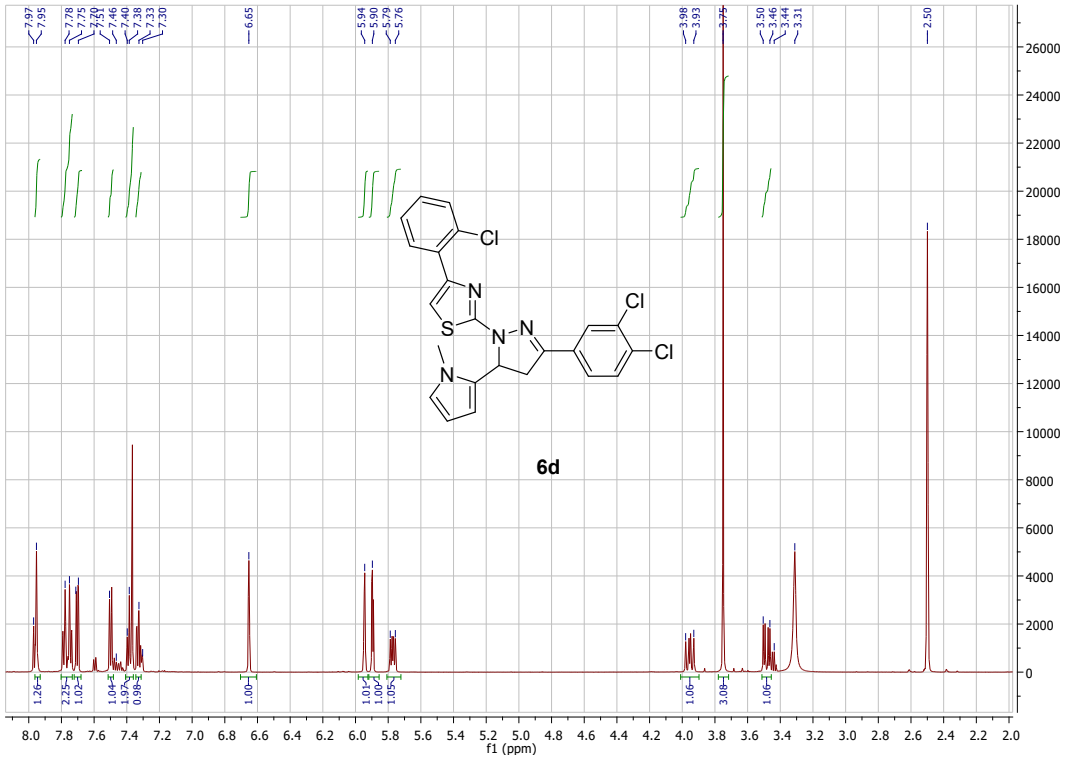

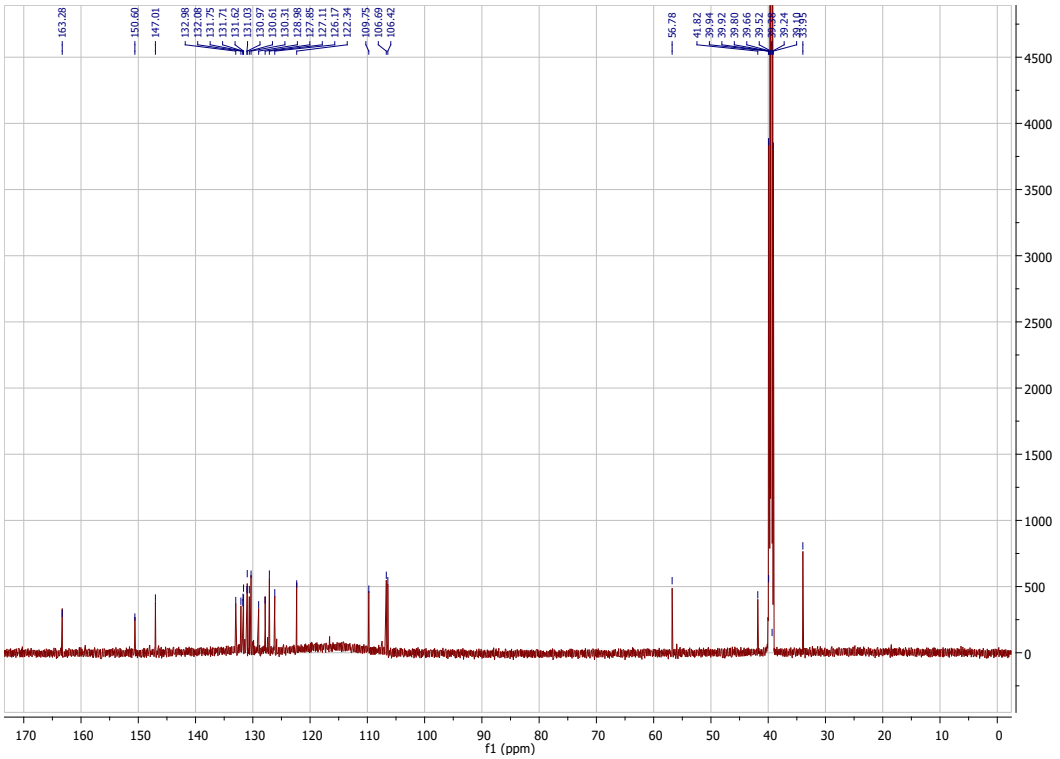

LC-MS spectra for 4-(2-chlorophenyl)-2-(3-(3,4-dichlorophenyl)-5-(1-methyl-1*H*-pyrrol-2-yl)-4,5-dihydro-1*H*-pyrazol-1-yl)thiazole **(6d)**.

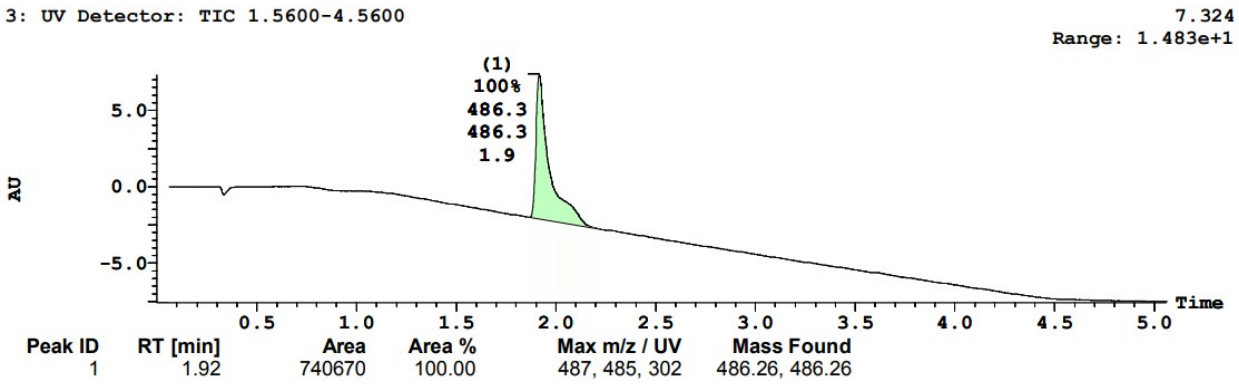

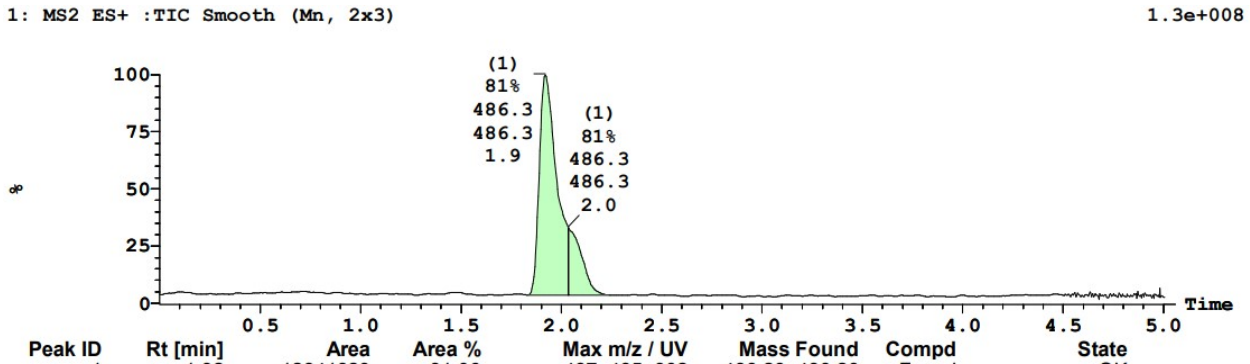

Peak ID	Rt [min]	Area	Area %	Max m/z / UV	Mass Found	Compd	State
1	1.92	12841829	81.06	487, 485, 302	486.26, 486.26	Found	OK
2	2.03	3000938	18.94	487	486.26	Found	OK

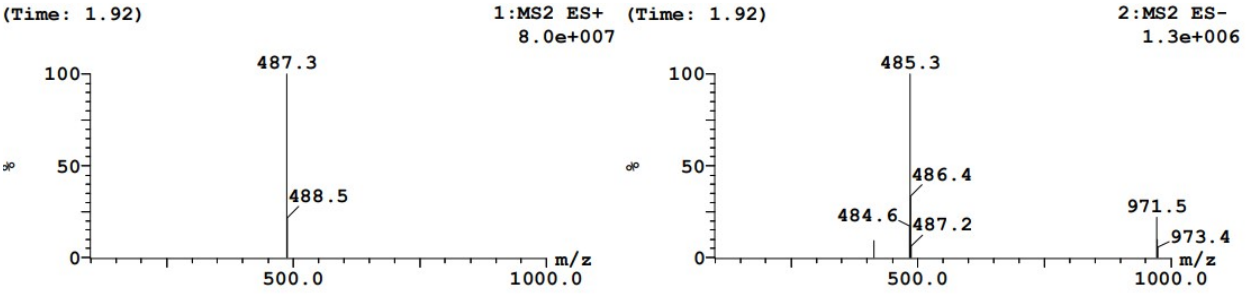

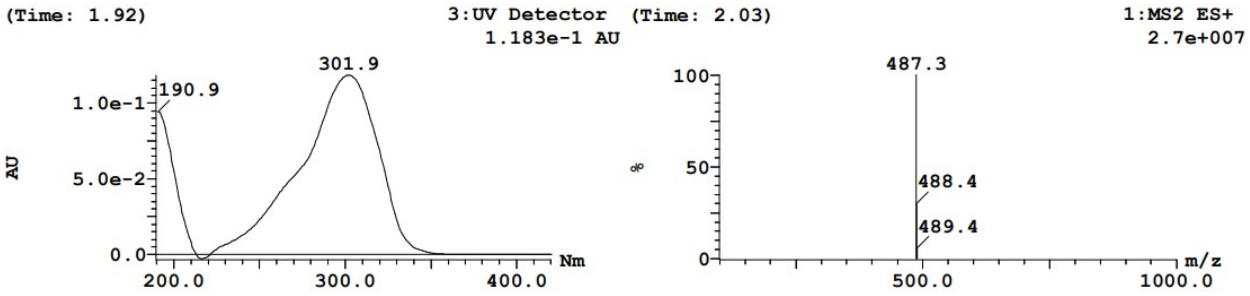

^{1}H and ^{13}C NMR spectra for 2-(3-(3,4-dichlorophenyl)-5-(1-methyl-1*H*-pyrrol-2-yl)-4,5-dihydro-1*H*-pyrazol-1-yl)-4-(1-phenyl-1*H*-pyrazol-4-yl)thiazole **(6e)**.

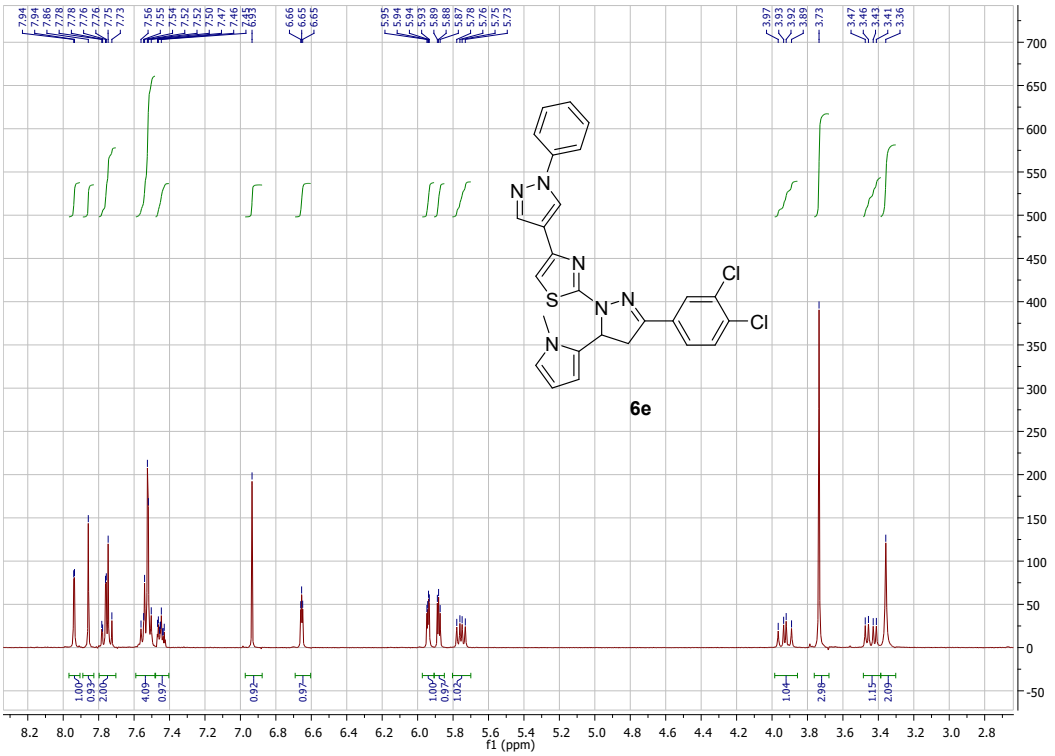

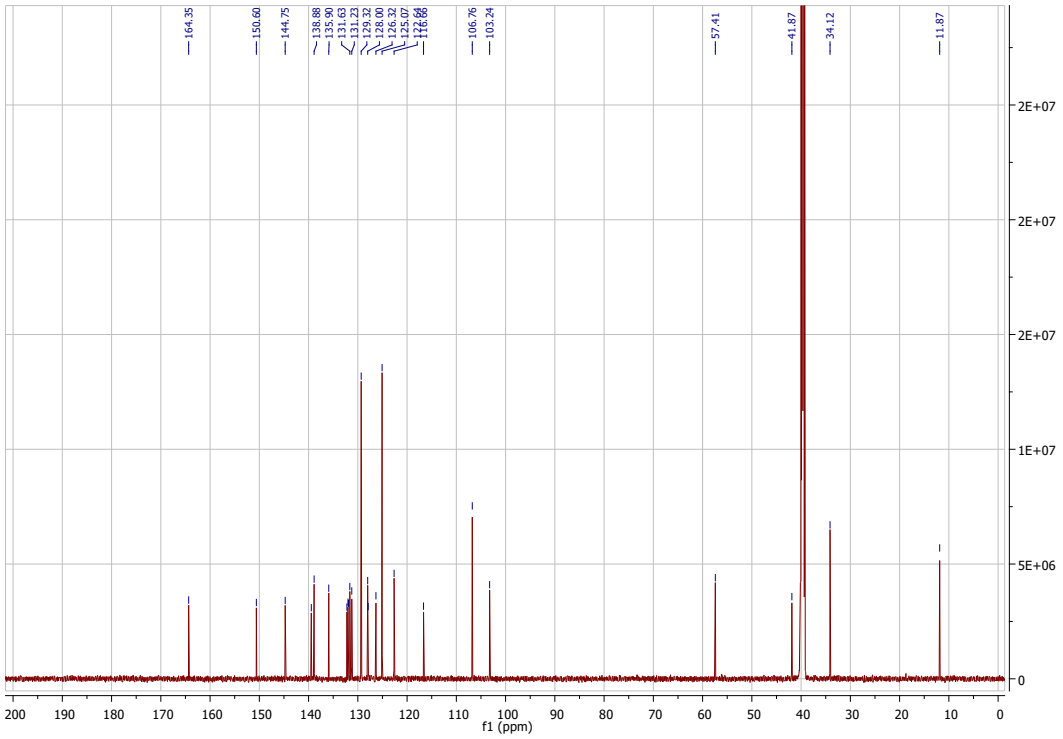

LC-MS spectra for 2-(3-(3,4-Dichlorophenyl)-5-(1-methyl-1*H*-pyrrol-2-yl)-4,5-dihydro-1*H*-pyrazol-1-yl)-4-(1-phenyl-1*H*-pyrazol-4-yl)thiazole (**6e**).

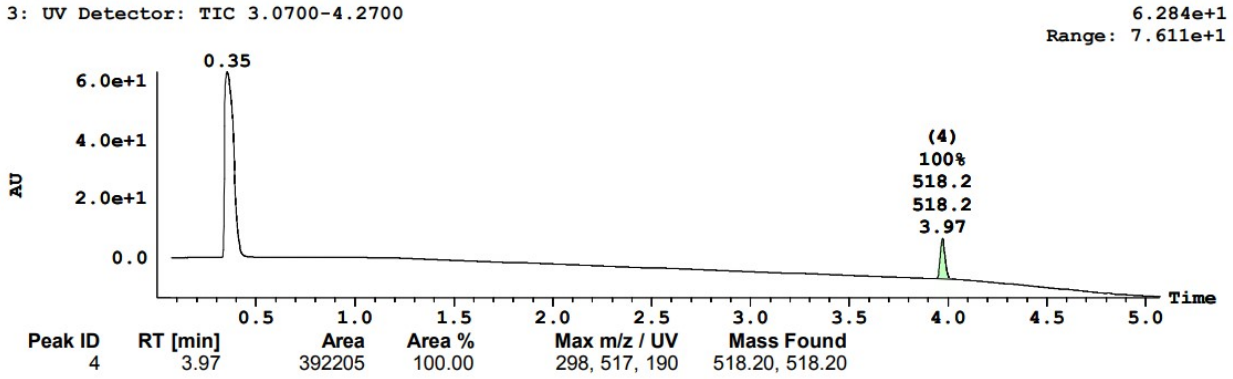

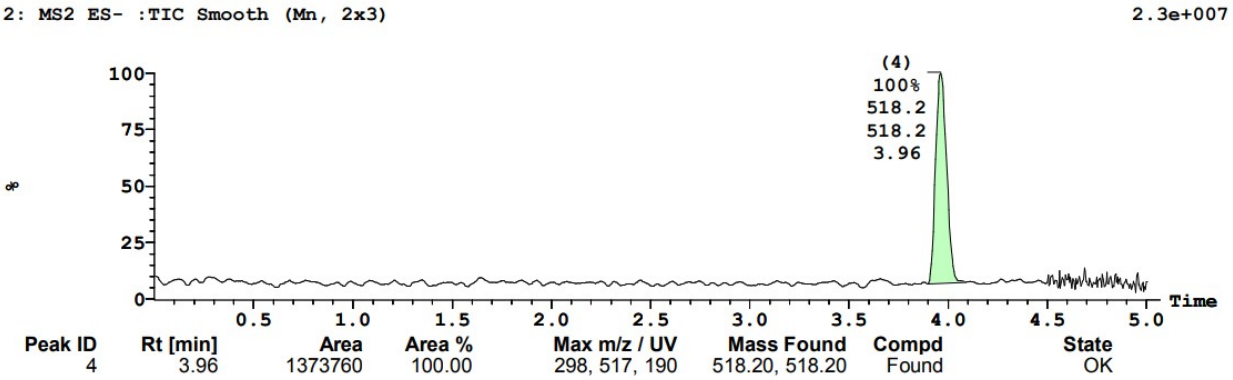

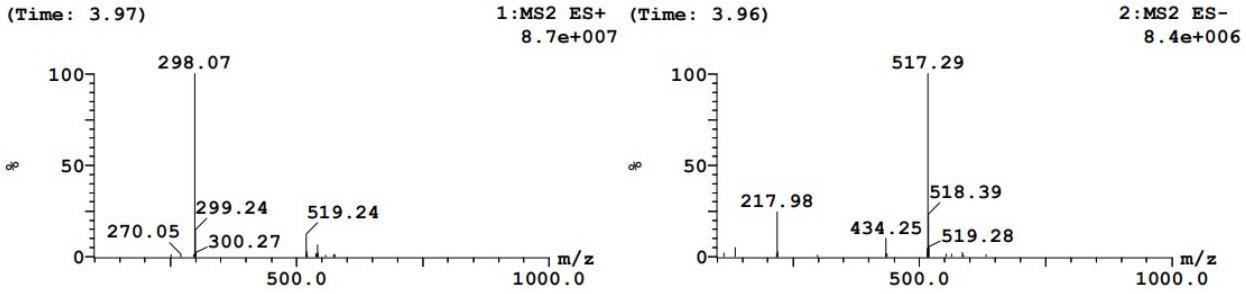

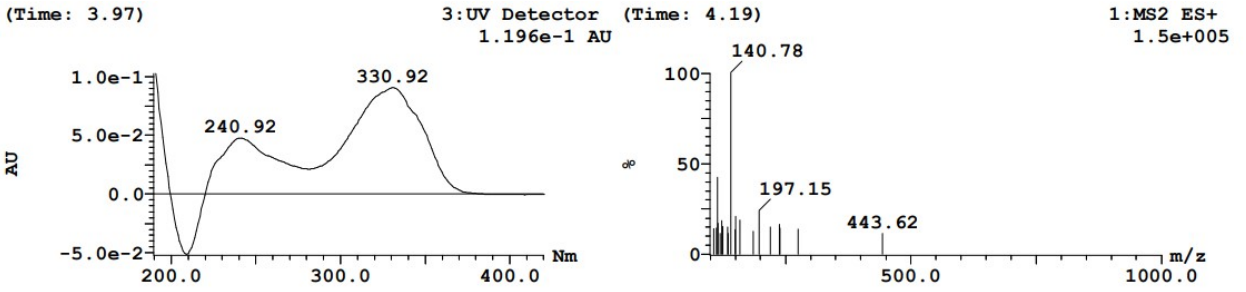

^{1}H and ^{13}C NMR spectra for ethyl 2-(3-(3,4-dichlorophenyl)-5-(1-methyl-1*H*-pyrrol-2-yl)-4,5-dihydro-1*H*-pyrazol-1-yl)thiazole-4-carboxylate **(7)**.

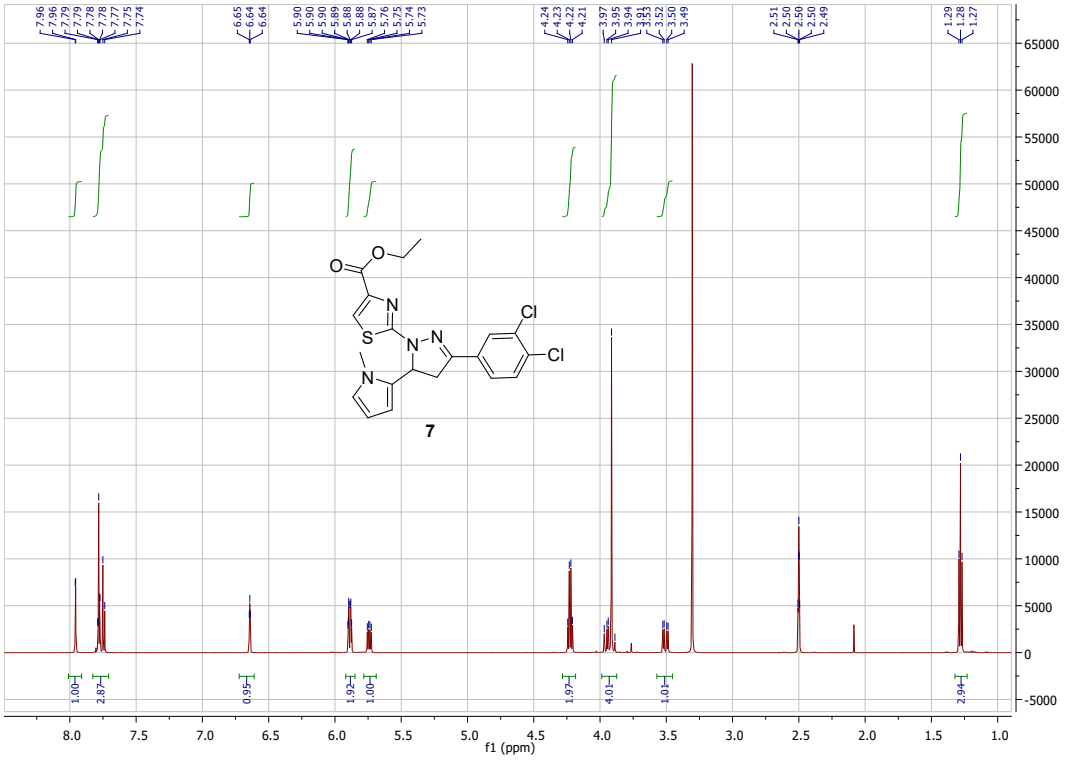

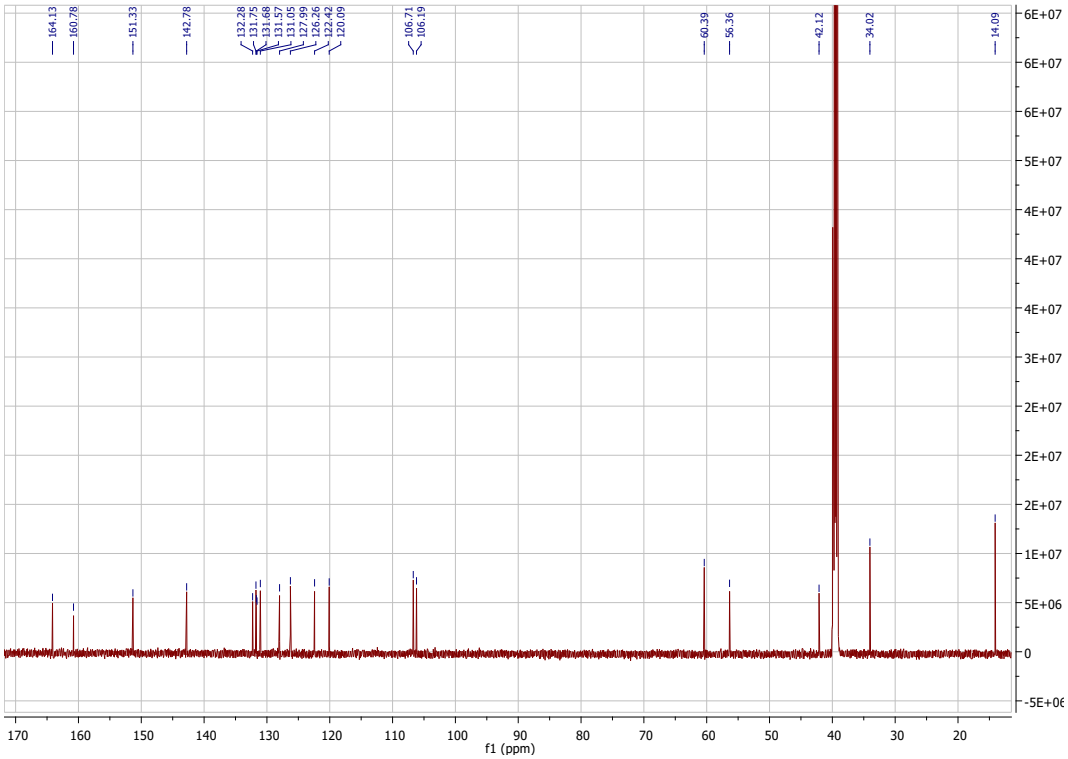

^{1}H and ^{13}C NMR spectra for 2-(3-(3,4-dichlorophenyl)-5-(1-methyl-1*H*-pyrrol-2-yl) -4,5-dihydro-1*H*-pyrazol-1-yl)thiazol -4-carbohydrazide **(8)**.

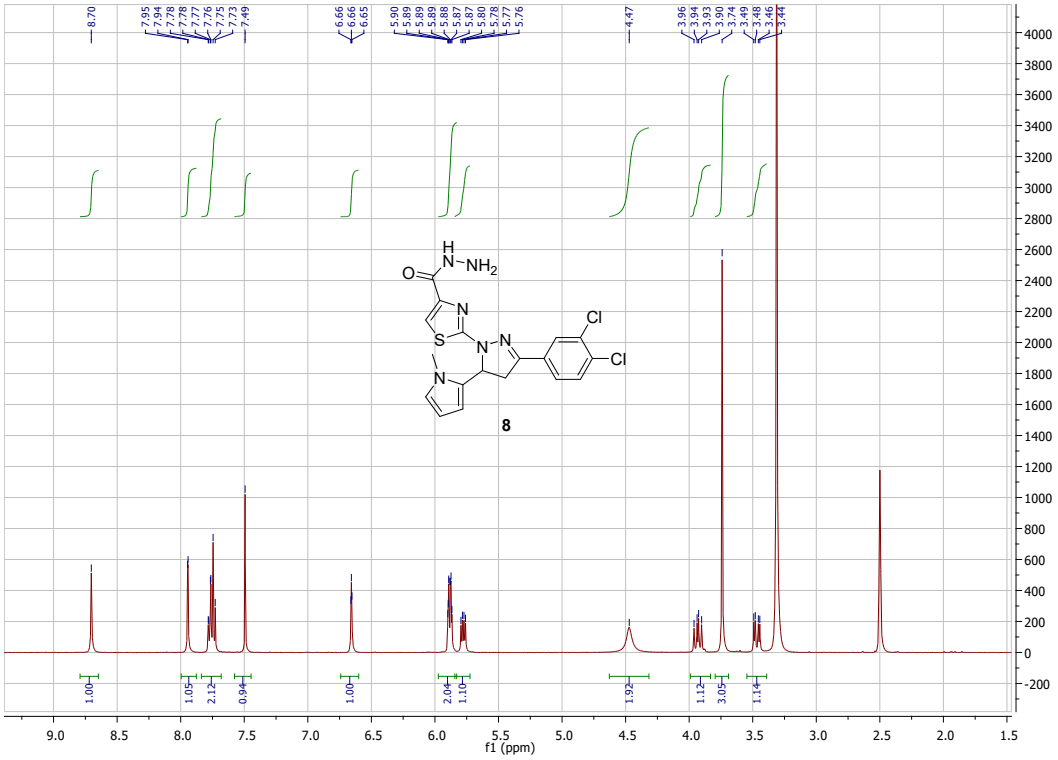

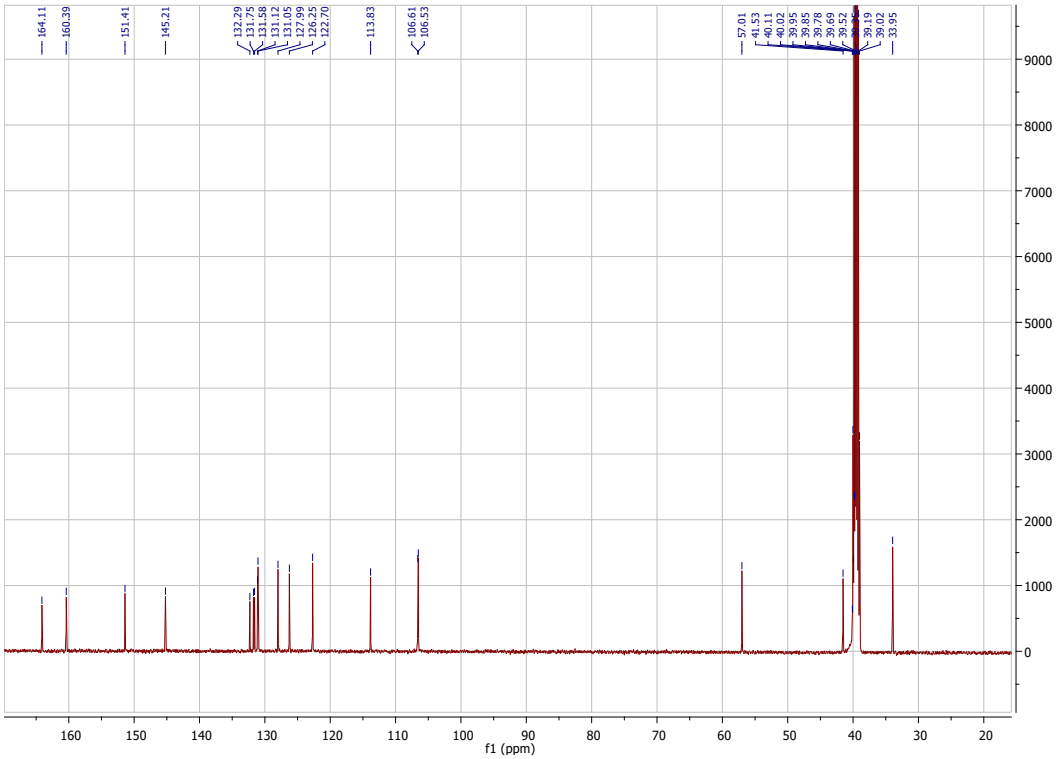

^{1}H and ^{13}C NMR spectra for 5-(2-(3-(3,4-dichlorophenyl)-5-(1-methyl-1*H*-pyrrol-2-yl) -4,5-dihydro-1*H*-pyrazol-1-yl)thiazol-4-yl)-1,3,4-oxadiazol-2-amine **(9).**

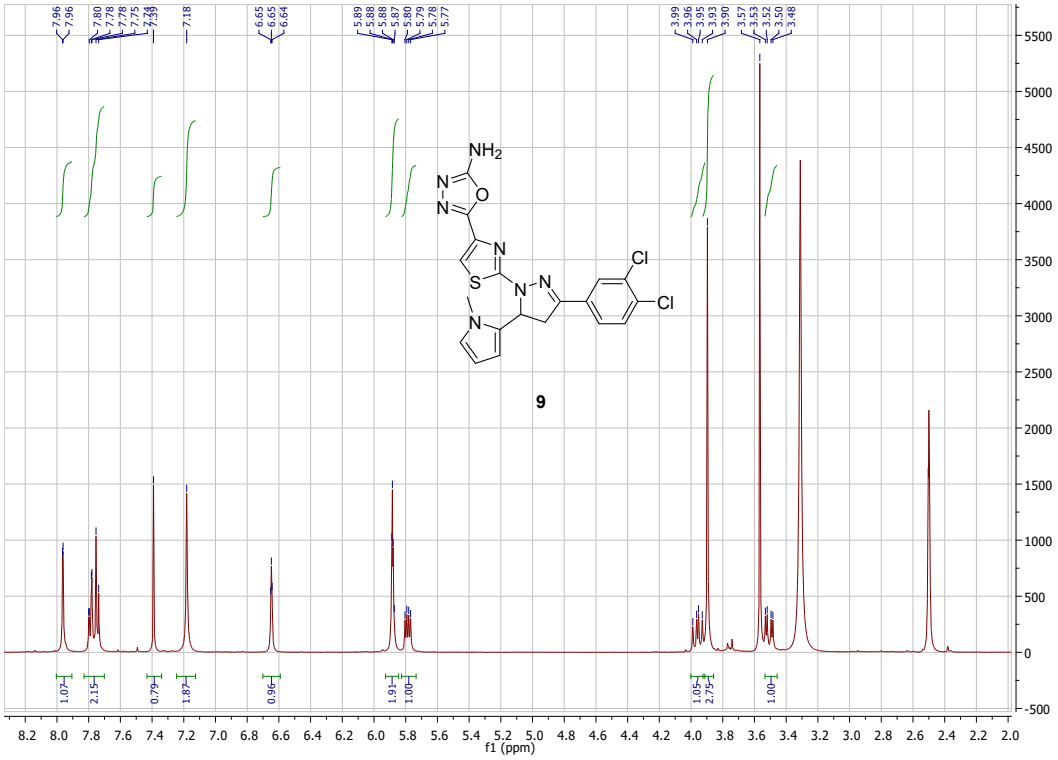

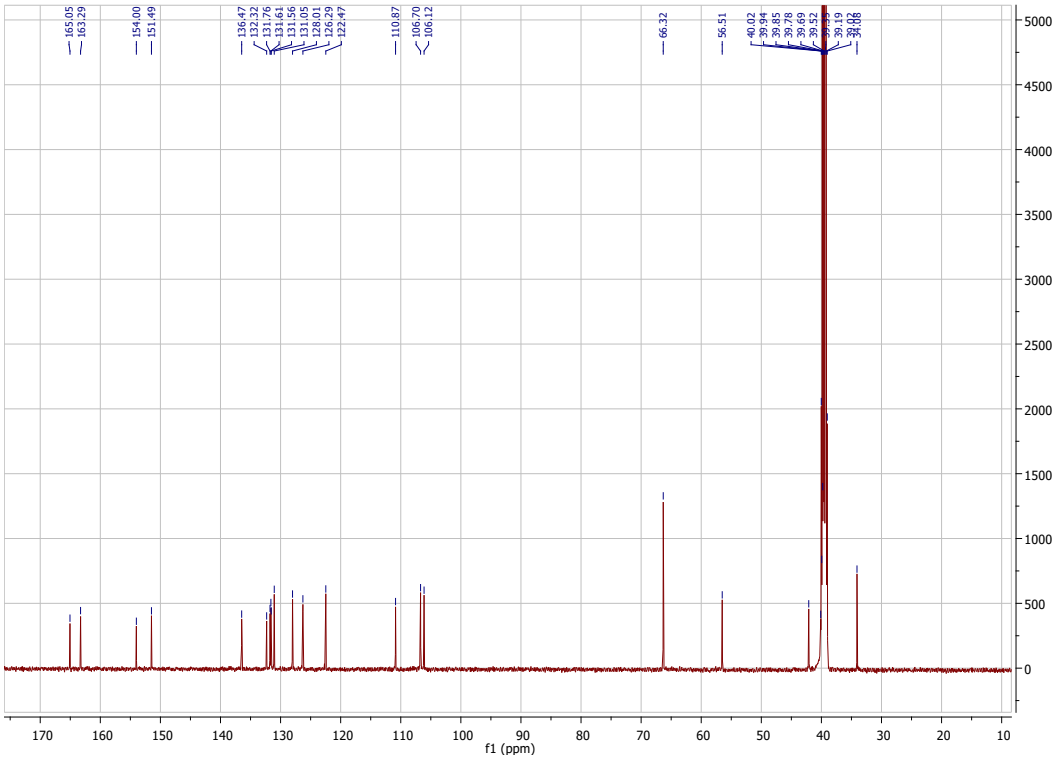

LC-MS spectra for 5-(2-(3-(3,4-dichlorophenyl)-5-(1-methyl-1*H*-pyrrol-2-yl)-4,5-dihydro-1*H*-pyrazol-1-yl)thiazol-4-yl)-1,3,4-oxadiazol-2-amine **(9)**.

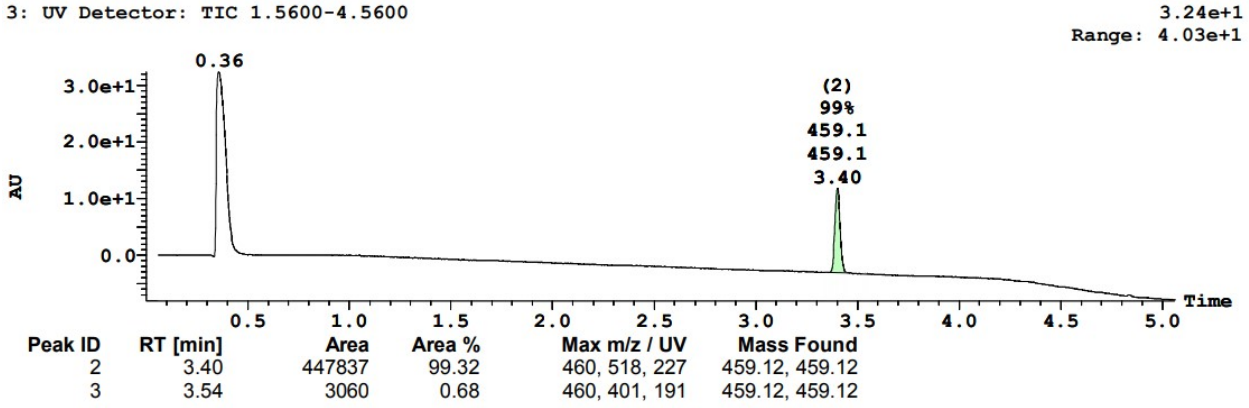

Peak ID	RT [min]	Area	Area %	Max m/z / UV	Mass Found
2	3.40	447837	99.32	460, 518, 227	459.12, 459.12
3	3.54	3060	0.68	460, 401, 191	459.12, 459.12

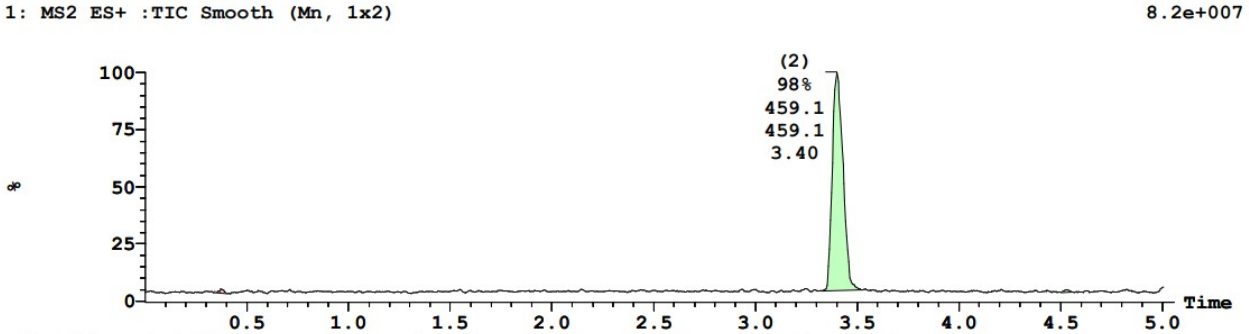

Peak ID	Rt [min]	Area	Area %	Max m/z / UV	Mass Found	Compd	State
1	0.37	42730	0.87	120			Diversity fail
2	3.40	4812949	98.47	460, 518, 227	459.12, 459.12	Found	OK
4	4.53	31919	0.65	199	459.12	Tentative	OK

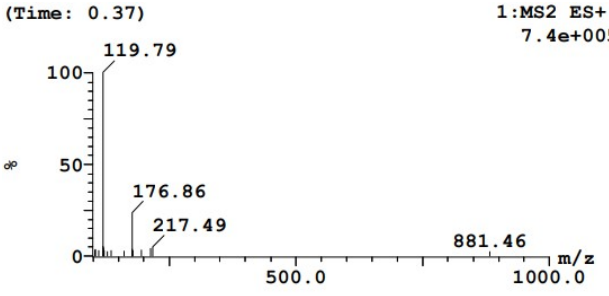

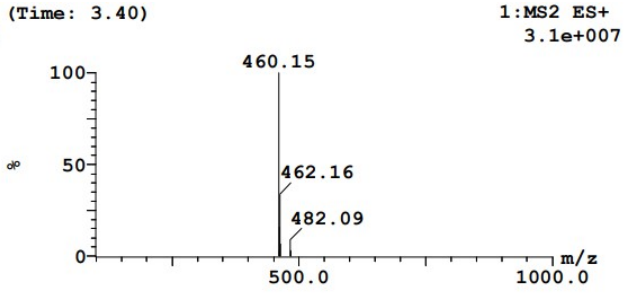

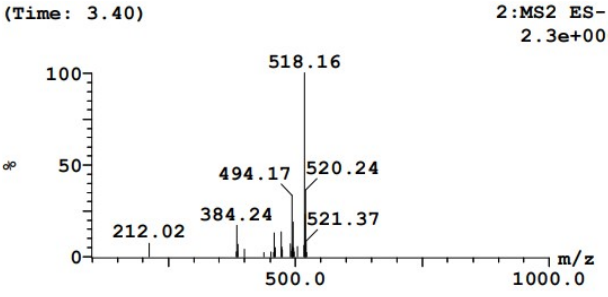

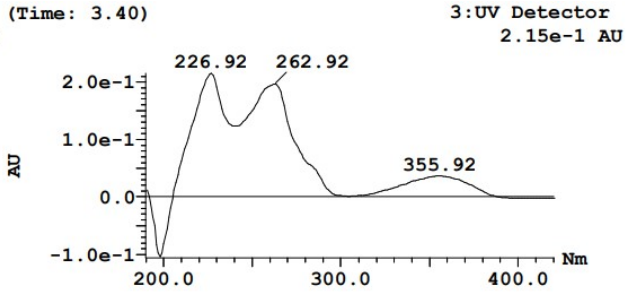

^{1}H and ^{13}C NMR spectra for N'-(2-(3-(3,4-dichlorophenyl)-5-(1-methyl-1*H*-pyrrol-2-yl)-4,5-dihydro -1*H*-pyrazol-1-yl)thiazole-4-carbonyl)-5-(dimethylamino)naphthalene-1-sulfonohydrazide **(10a).**

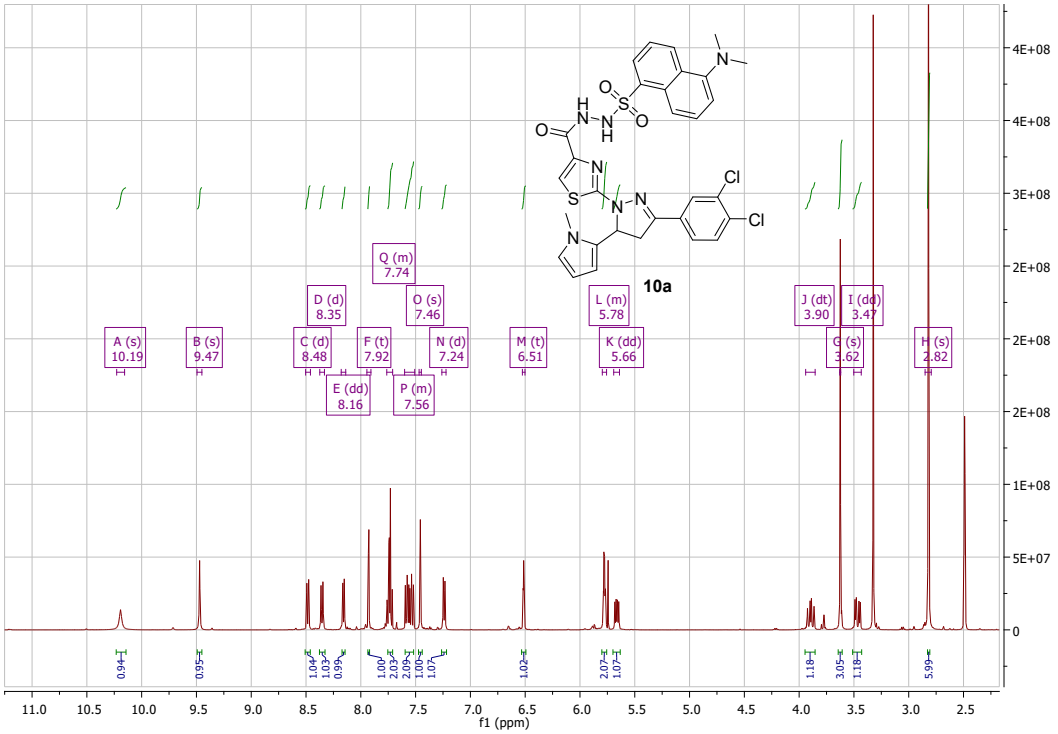

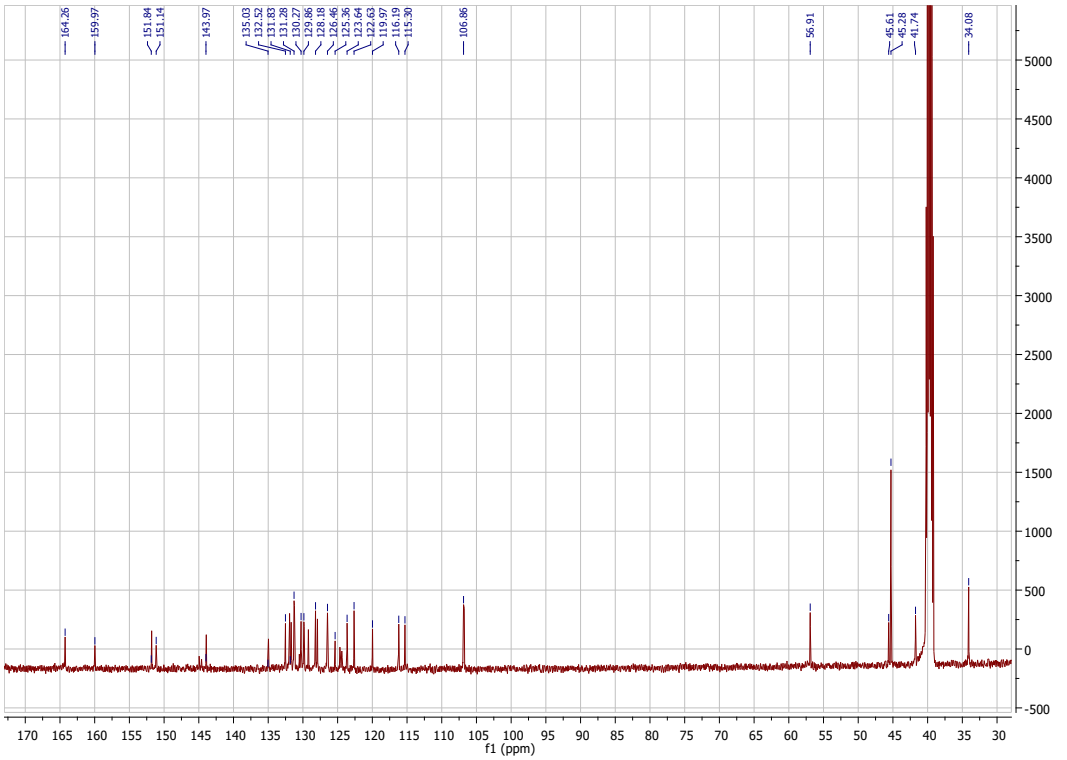

^{1}H and ^{13}C NMR spectra for N'-(2-(3-(3,4-dichlorophenyl)-5-(1-methyl-1*H*-pyrrol-2-yl) -4,5-dihydro-1*H*-pyrazol-1-yl)thiazole-4-carbonyl)-4-fluorobenzenesulfonohydrazide **(10b).**

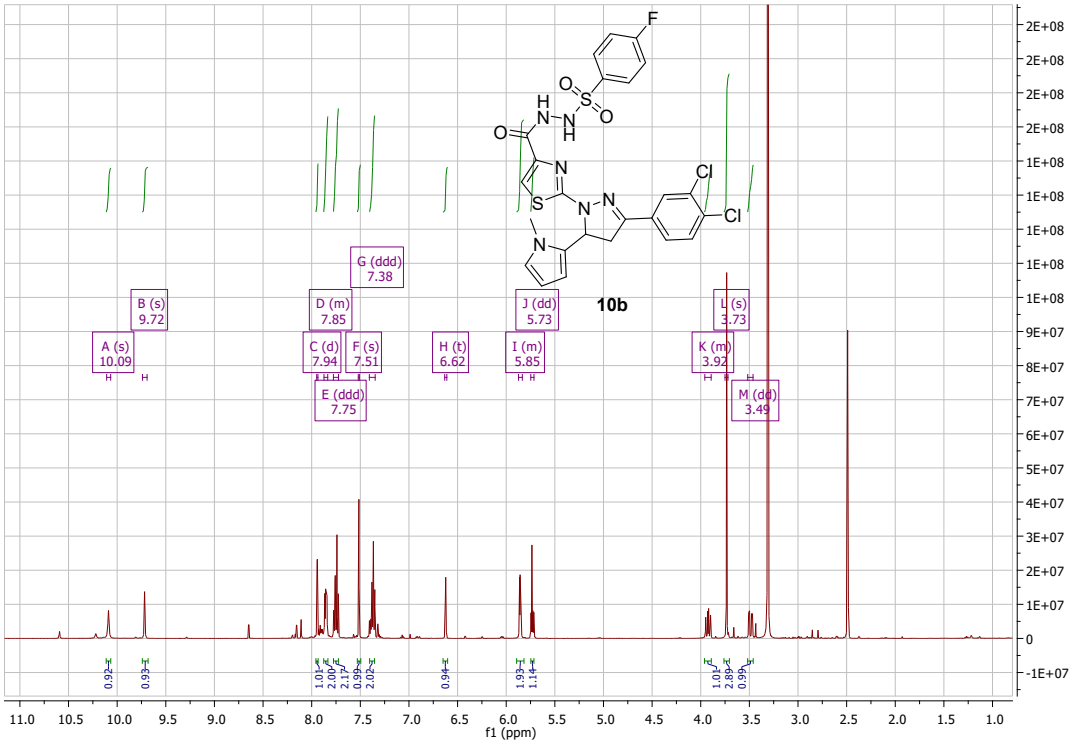

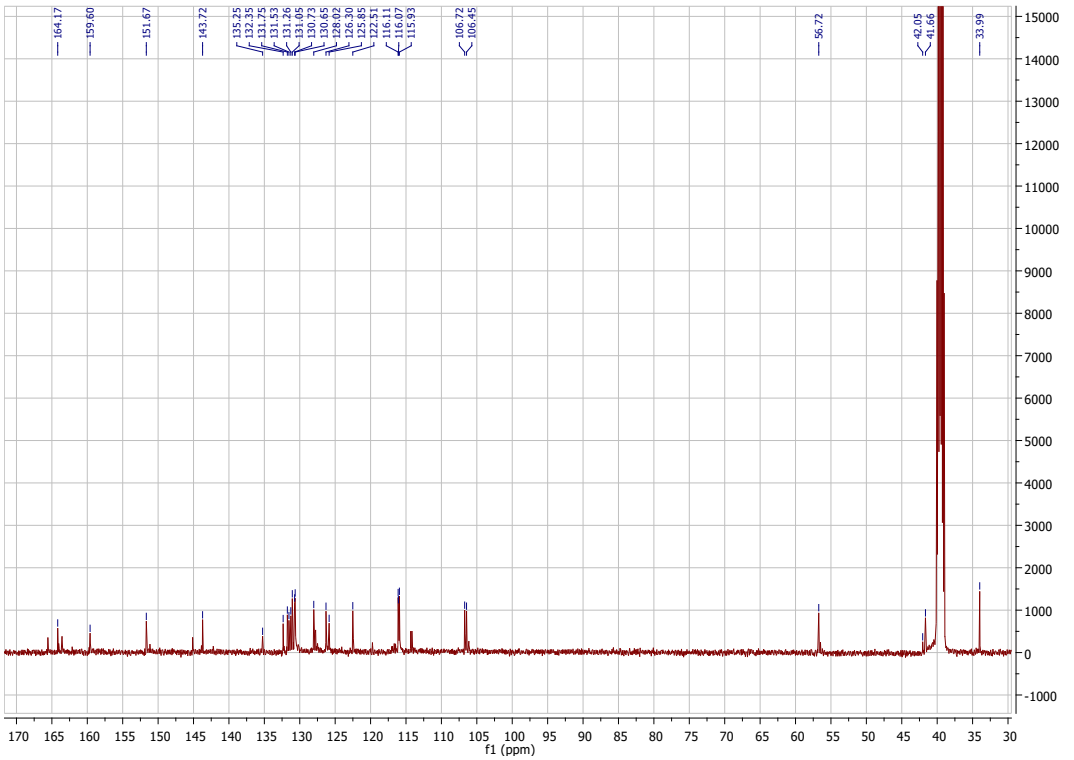

LC-MS spectra for N'-(2-(3-(3,4-dichlorophenyl)-5-(1-methyl-1*H*-pyrrol-2-yl) -4,5-dihydro-1*H*-pyrazol-1-yl)thiazole-4-carbonyl)-4-fluorobenzenesulfonohydrazide **(10b)**.

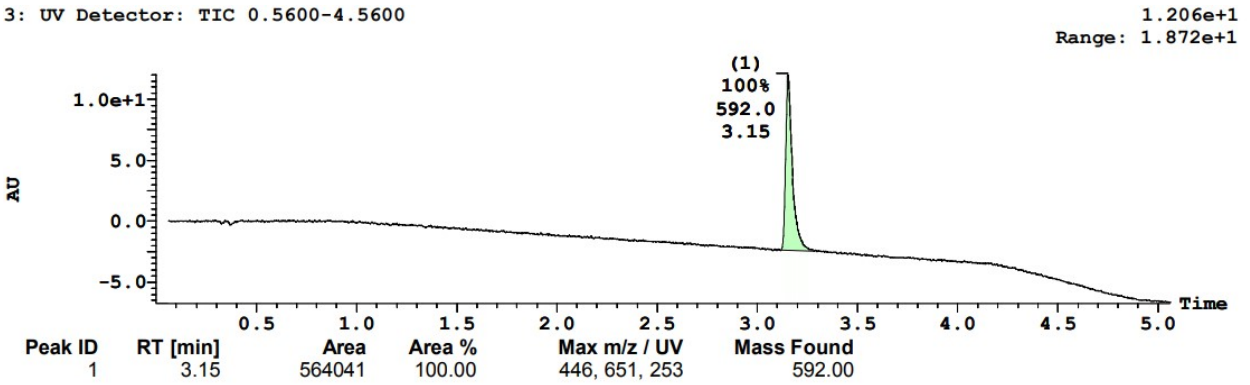

Peak ID	RT [min]	Area	Area %	Max m/z / UV	Mass Found
1	3.15	564041	100.00	446, 651, 253	592.00

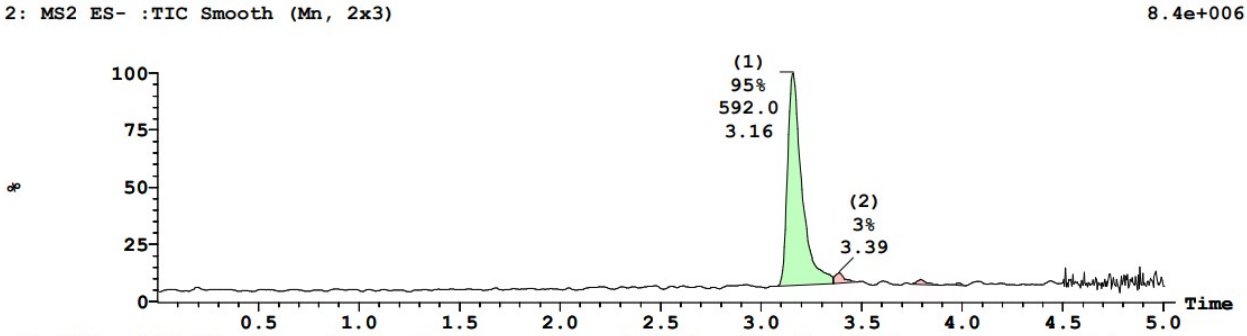

Peak ID	Rt [min]	Area	Area %	Max m/z / UV	Mass Found	Compd	State
1	3.16	651348	94.94	446, 651, 253	592.00	Found	Diversity fail
2	3.39	20976	3.06	212			Diversity fail
3	3.79	10623	1.55	744			Diversity fail
4	3.98	3119	0.45	213			Diversity fail

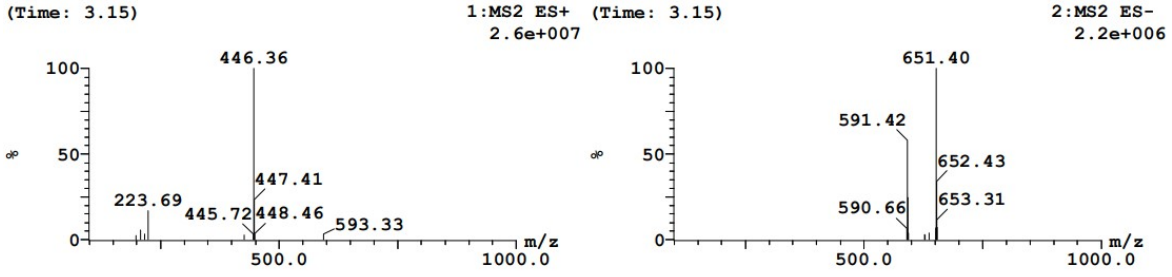

Peak ID	Target	Mass Found
1	No Target	

Peak ID	Target	Mass Found
2	592.0,591.0	

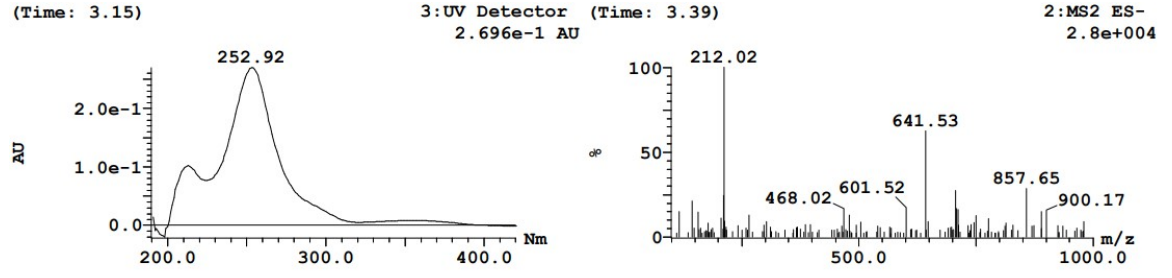

Peak ID	Target	Mass Found
3	592.0,591.0	

Peak ID	Target	Mass Found
4	592.0,591.0	

^{1}H and ^{13}C NMR spectra for N'-(2-(3-(3,4-Dichlorophenyl)-5-(1-methyl-1*H*-pyrrol-2-yl)- 4,5-dihydro-1*H*-pyrazol-1-yl)thiazole-4-carbonyl)butane-1-sulfonohydrazide **(10c).**

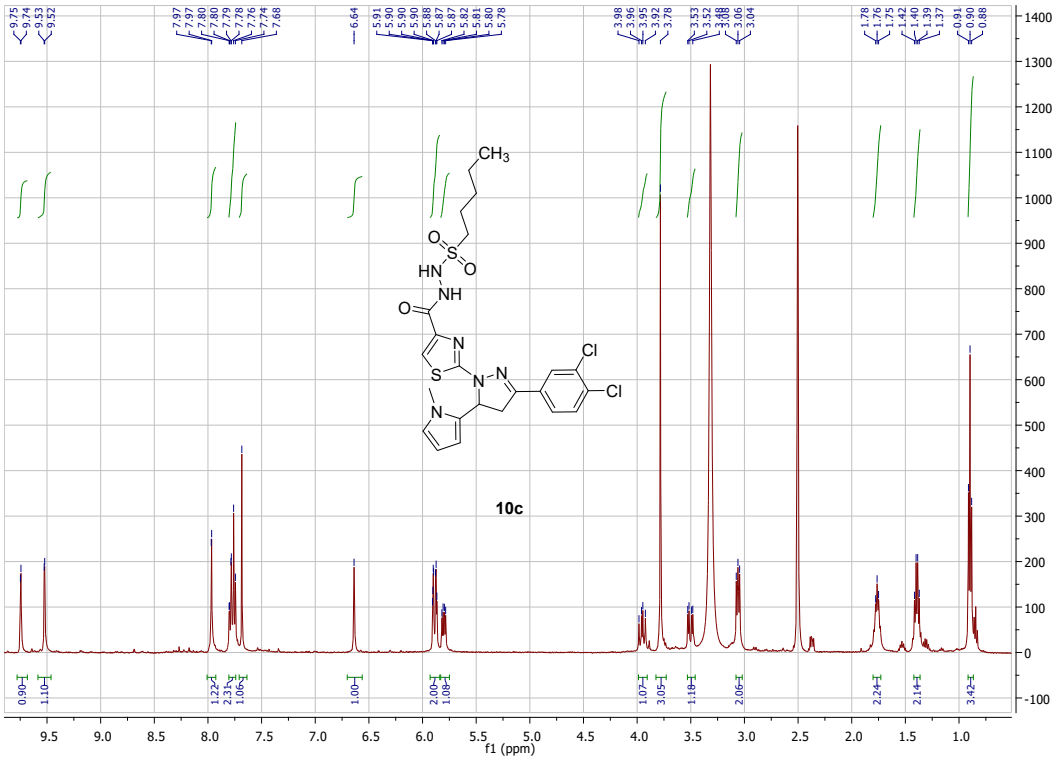

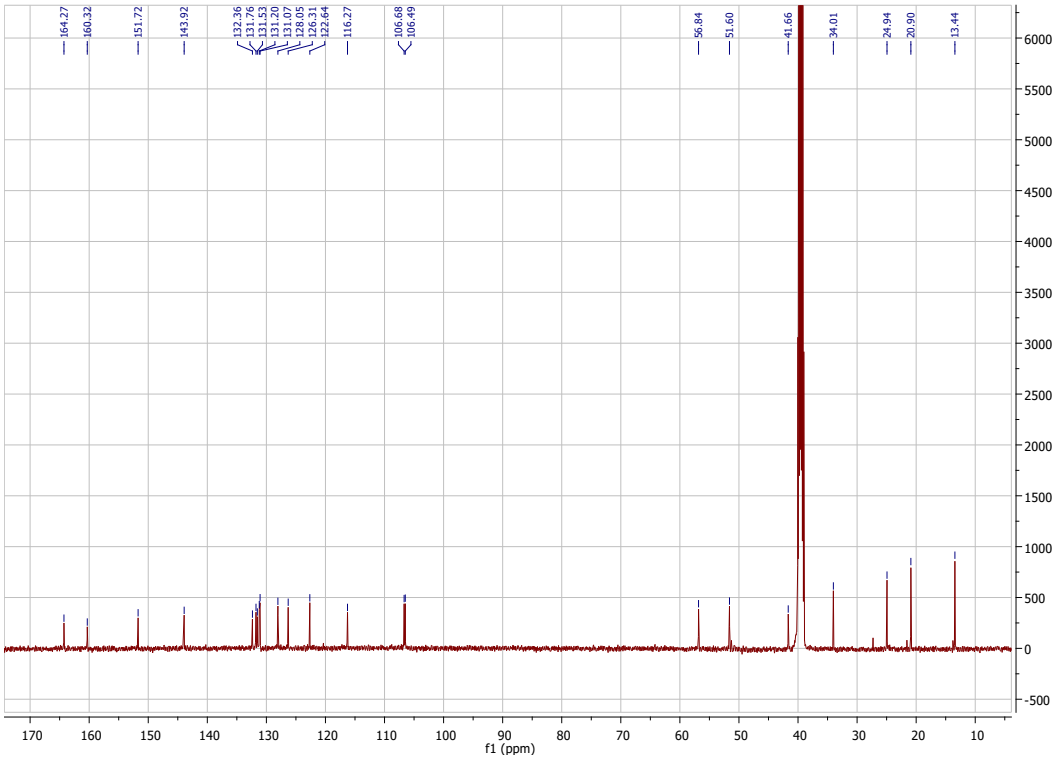

LC-MS spectra for N'-(2-(3-(3,4-Dichlorophenyl)-5-(1-methyl-1*H*-pyrrol-2-yl)-4,5-dihydro-1*H*-pyrazol-1-yl)thiazole-4-carbonyl)butane-1-sulfonohydrazide **(10c)**.

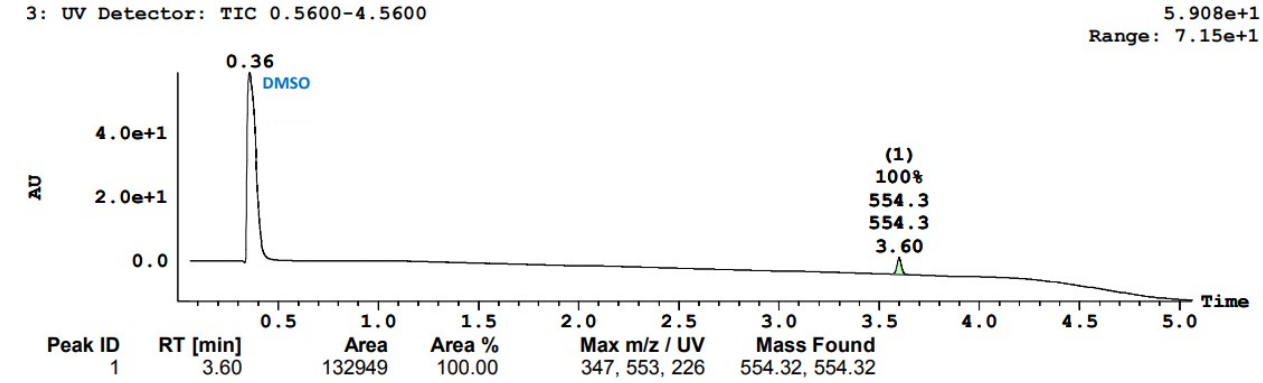

Peak ID	RT [min]	Area	Area %	Max m/z / UV	Mass Found
1	3.60	132949	100.00	347, 553, 226	554.32, 554.32

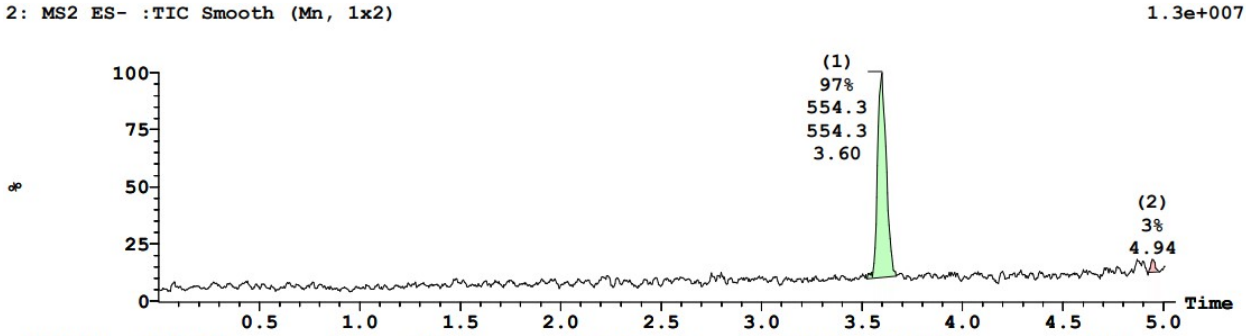

Peak ID	Rt [min]	Area	Area %	Max m/z / UV	Mass Found	Compd	State
1	3.60	560524	97.06	347, 553, 226	554.32, 554.32	Found	OK
2	4.94	16966	2.94	212			Diversity fail

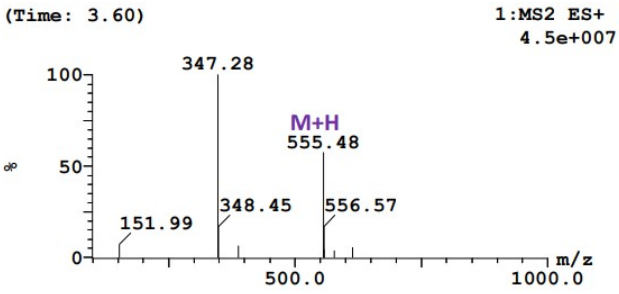

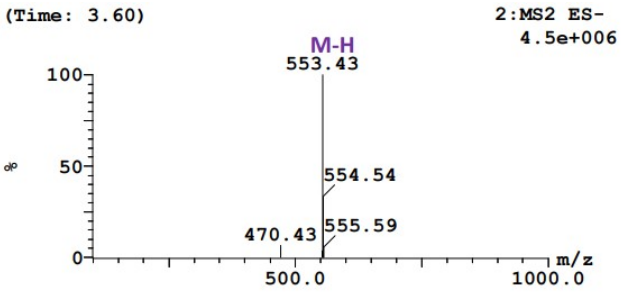

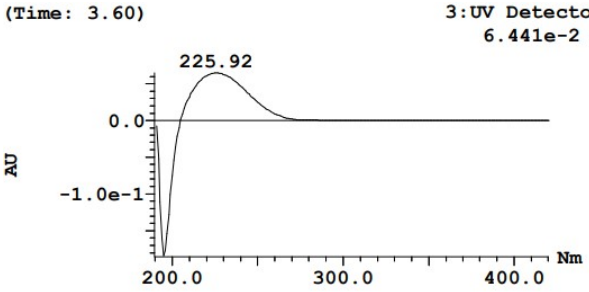

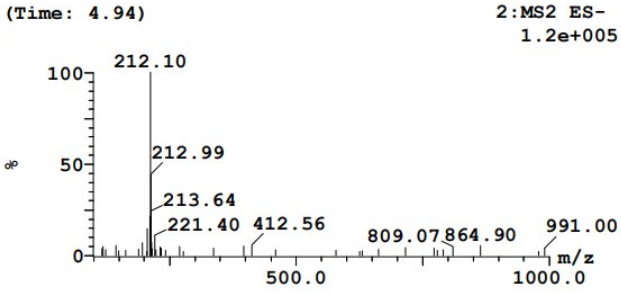

^{1}H and ^{13}C NMR spectra for 2-(3-(3,4-dichlorophenyl)-5-(1-methyl-1*H*-pyrrol-2-yl) -4,5-dihydro-1*H*-pyrazol-1-yl)thiazol-4(5*H*)-one **(11).**

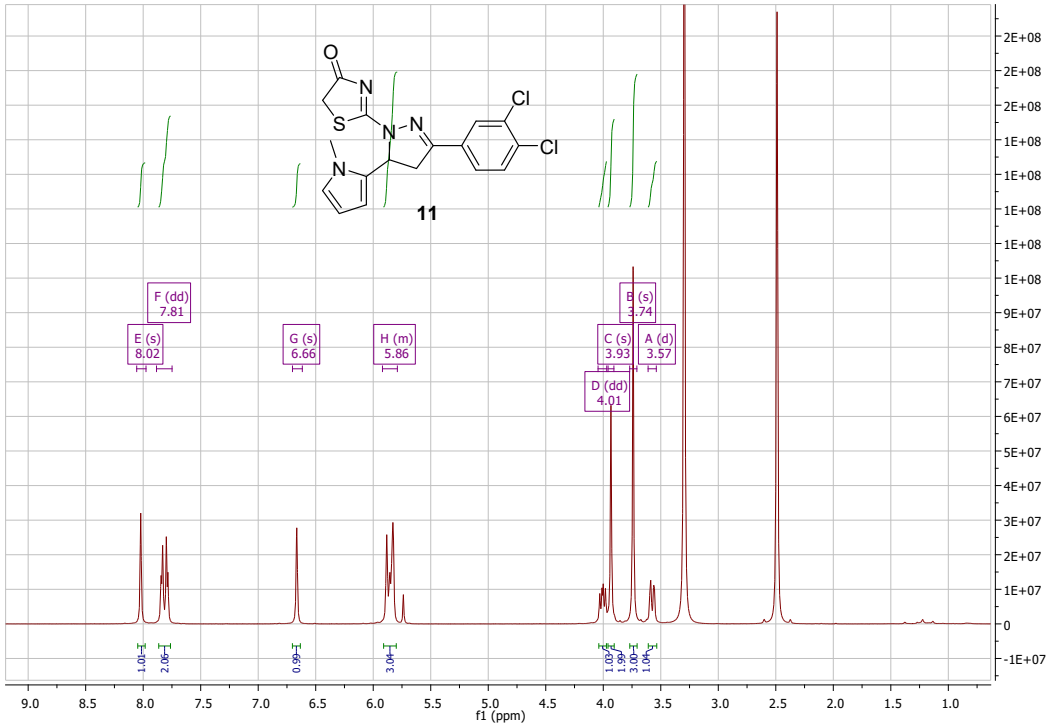

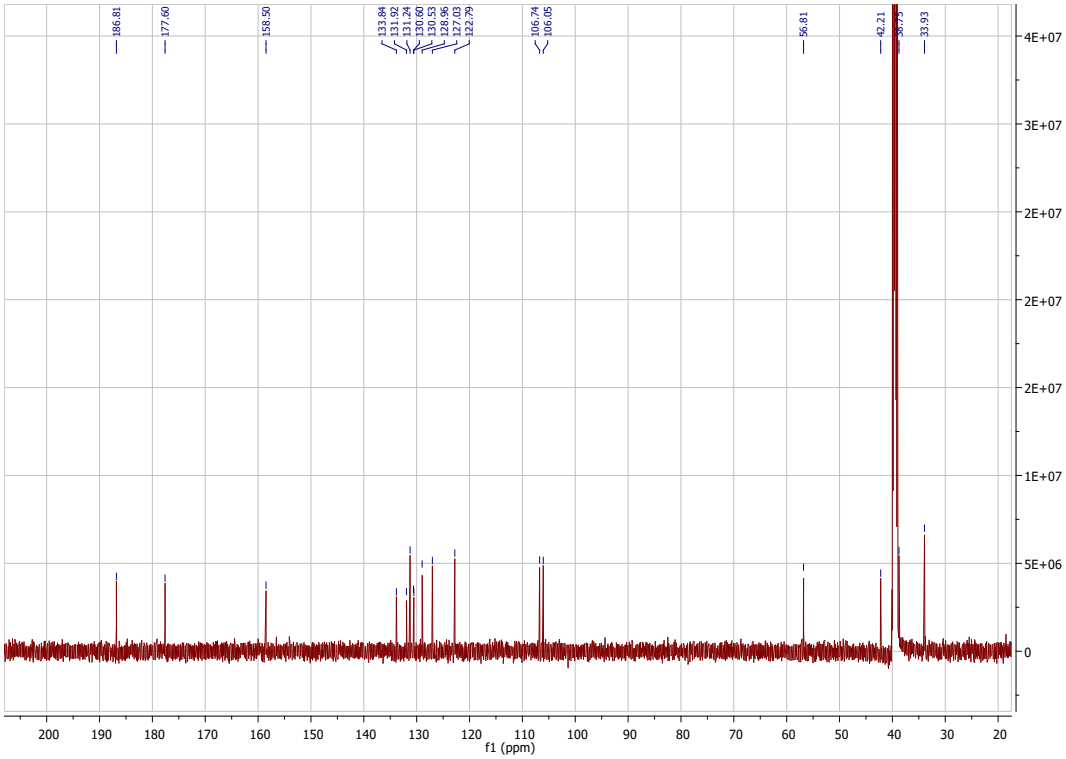

LC-MS spectra for 2-(3-(3,4-dichlorophenyl)-5-(1-methyl-1*H*-pyrrol-2-yl) -4,5-dihydro-1*H*-pyrazol-1-yl)thiazol-4(5*H*)-one **(11).**

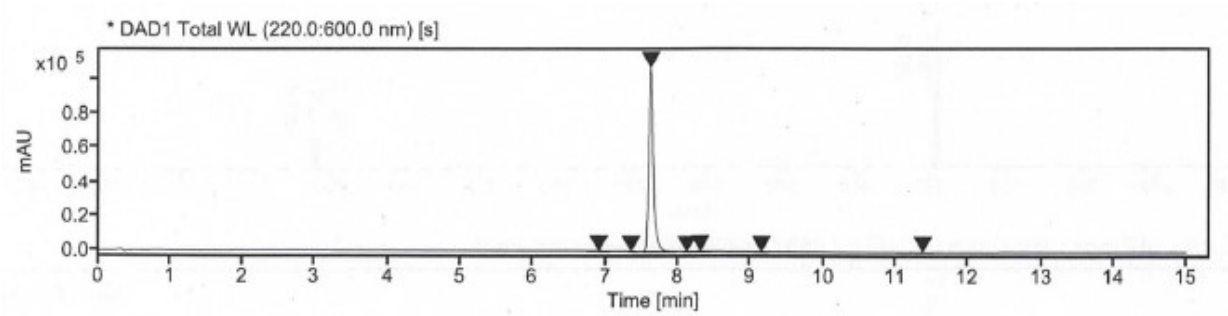

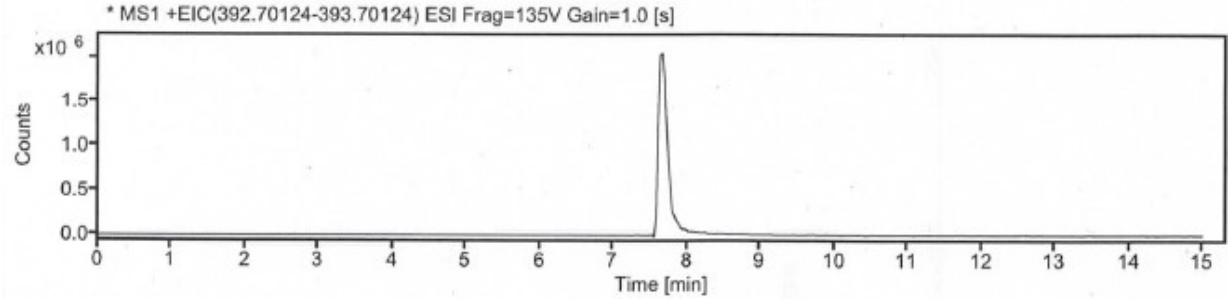

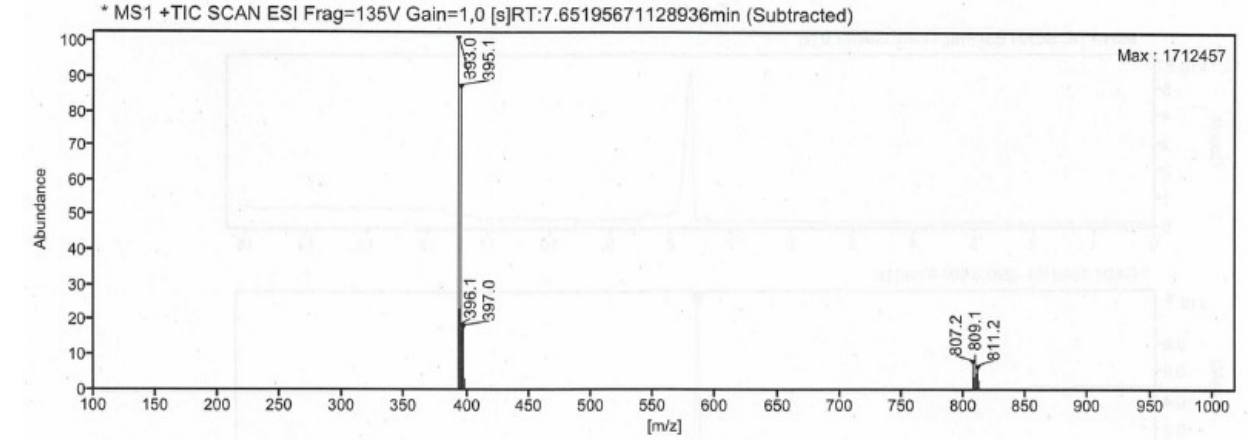

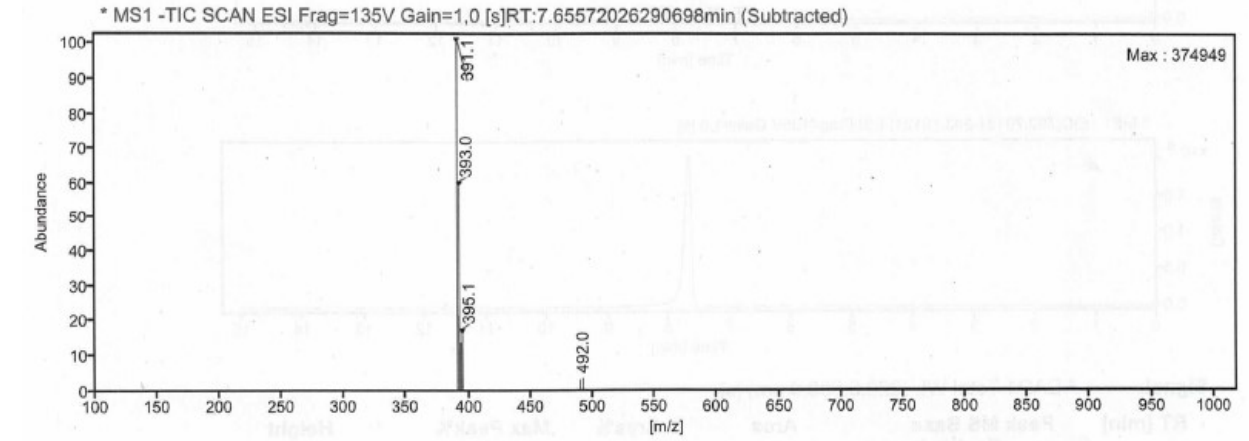

Signal: * DAD1 Total WL (220.0:600.0 nm) [s]

RT [min]	Peak MS Base Peak m/z	Area	Area%	Max Peak%	Height
6.906		274.6319	0.0557	0.056	28.285
7.352		429.5547	0.0871	0.088	112.934
7.622		489803.3919	99.3038	100.000	107155.077
8.121		79.5742	0.0161	0.016	28.800
8.306		1859.5886	0.3770	0.380	394.006
9.151		179.7776	0.0364	0.037	40.970
11.378		610.6246	0.1238	0.125	41.068

^{1}H and ^{13}C NMR spectra for (E)-2-(3-(3,4-dichlorophenyl)-5-(1-methyl-1*H*-pyrrol-2-yl)-4,5 -dihydro-1*H*-pyrazol-1-yl)-5-(4-fluorobenzylidene)thiazol-4(5*H*)-one **(12a)**.

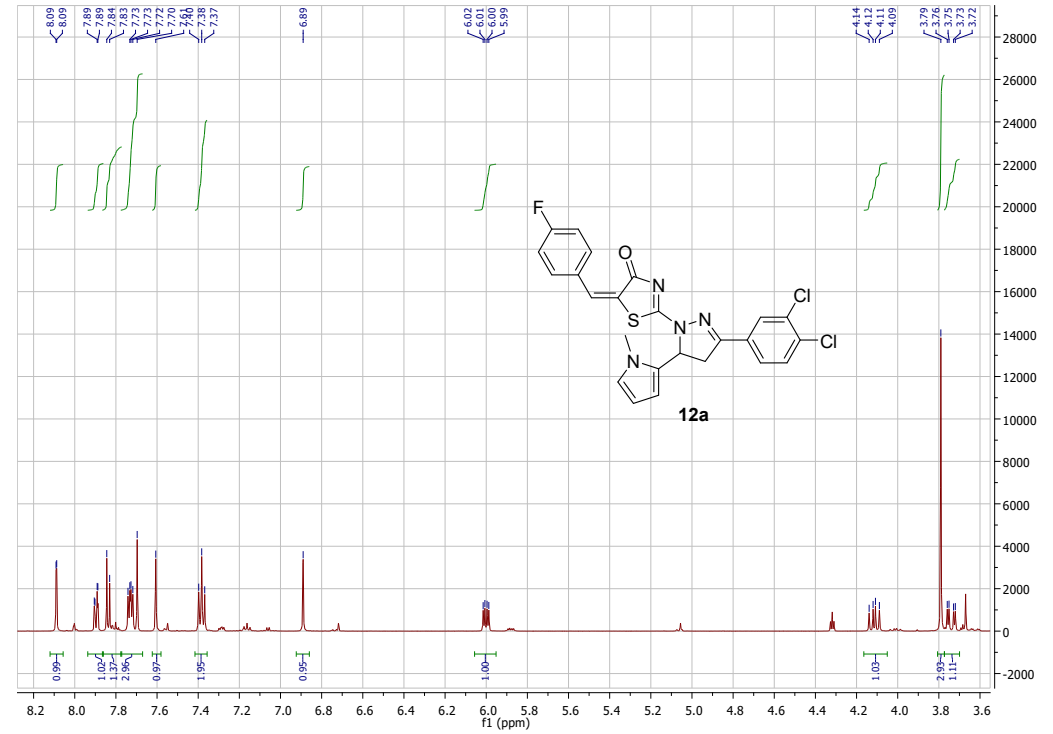

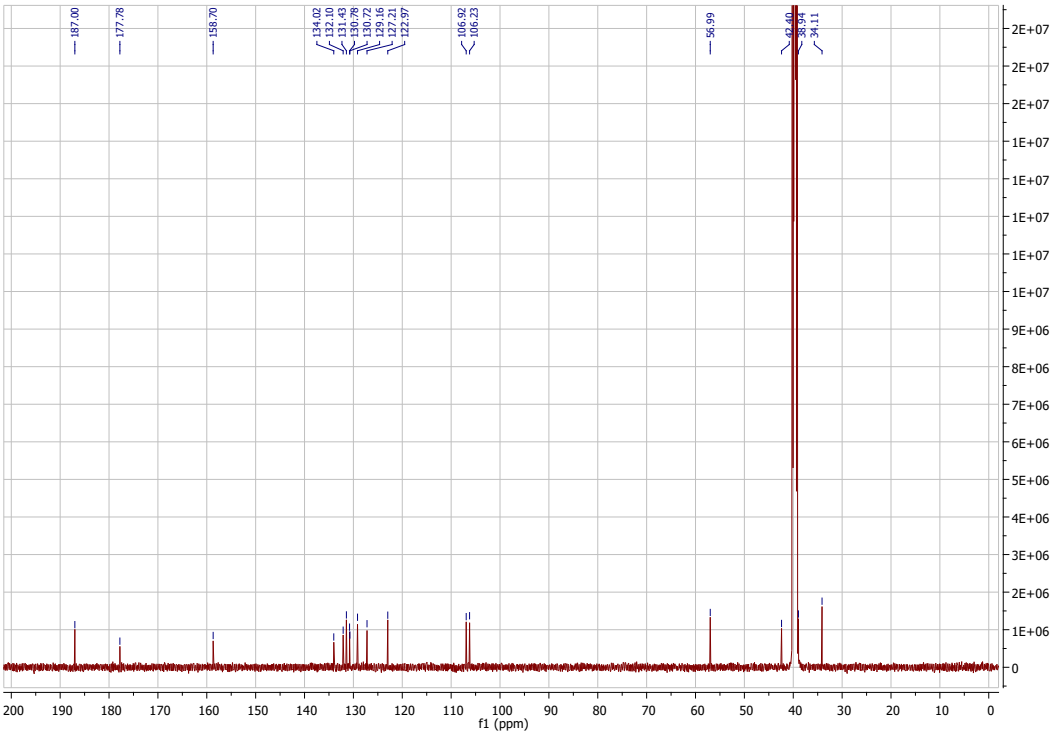

^{1}H and ^{13}C NMR spectra for (E)-5-(3-chloro-4-fluorobenzylidene)-2-(3-(3,4-dichlorophenyl)-5 -(1-methyl-1*H*-pyrrol-2-yl)-4,5-dihydro-1*H*-pyrazol-1-yl)thiazol-4(5*H*)-one **(12c)**.

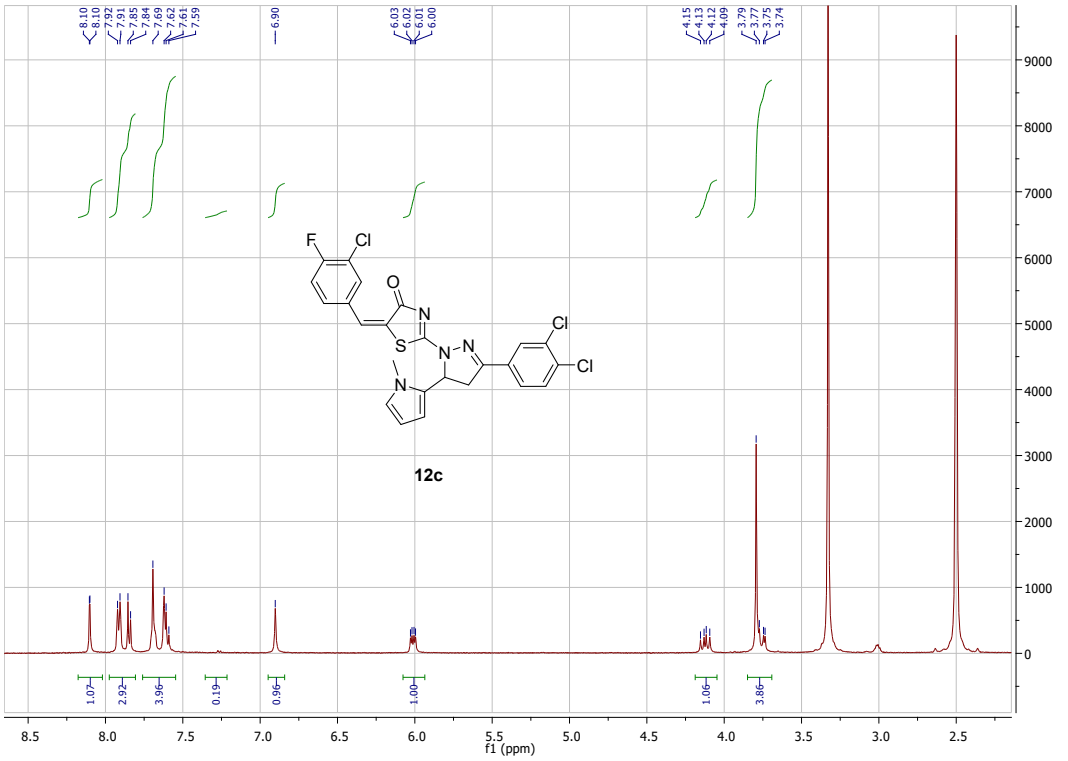

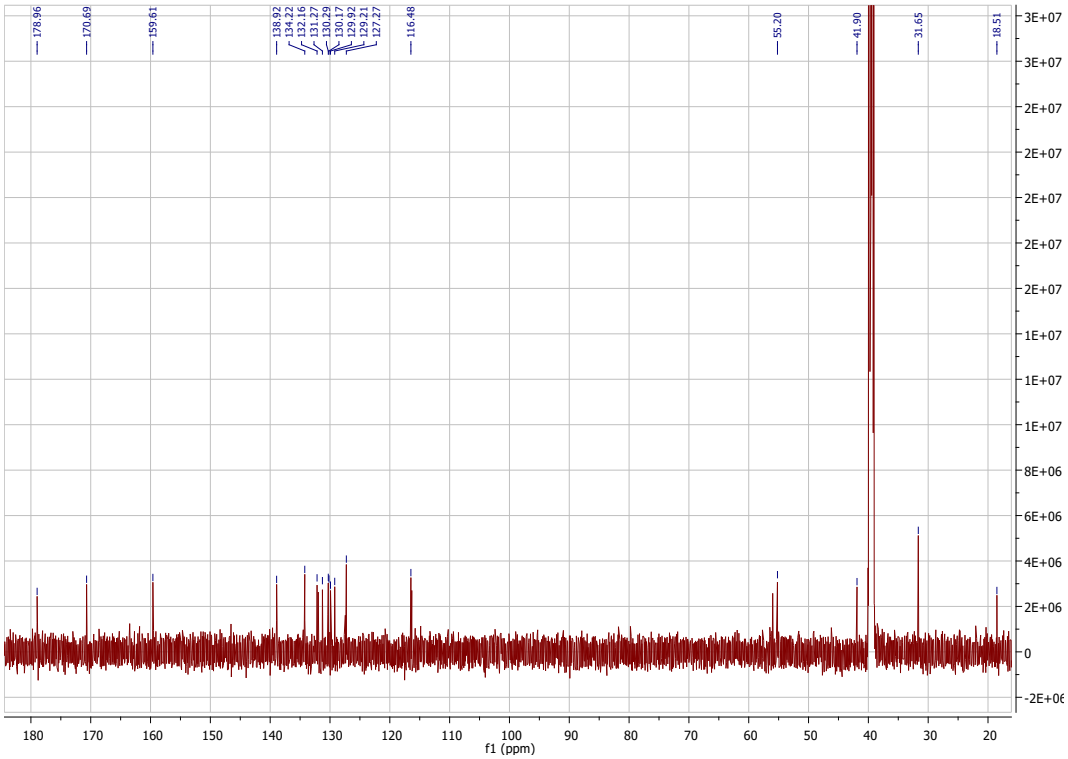

References

1. Perez, H. L., Banfi, P., Bertrand, J., Cai, Z. W., Grebinski, J. W., Kim, K., Lippy, J., Modugno, M., Naglich, J., Schmidt, R. J., Tebben, A., Vianello, P., Wei, D. D., Zhang, L., Galvani, A., Lombardo, L. J., Borzilleri, R. M. Identification of a phenylacylsulfonamide series of dual Bcl-2/Bcl-xL antagonists. Bioorganic & Medicinal Chemistry Letters **2012**, *22*, 3946-3950.
2. BIOVIA, Dassault Systèmes, BIOVIA Discovery Studio Visualizer, 2021, San Diego: Dassault Systèmes, **2023**. https://www.3ds.com/
3. Morris, G. M., Huey, R., Lindstrom, W., Sanner, M. F., Belew, R. K., Goodsell, D. S., Olson, A. J. AutoDock4 and AutoDockTools4: Automated docking with selective receptor flexibility. Journal of Computational Chemistry **2009**, *30*, 2785-2791.